Heterogeneous Gold-Based Catalysis for Green Chemistry: Low-Temperature CO Oxidation and Propene Oxidation

Byoung Koun Min[†,‡] and Cynthia M. Friend*[,†,§]

Department of Chemistry and Chemical Biology and Division of Engineering and Applied Sciences, Harvard University, 12 Oxford Street, Cambridge, Massachusetts 02138

Received August 17, 2006

Contents

1. Introduction

Due to increasing concern about environmental impact, there has been tremendous recent interest in developing new processes that both reduce energy consumption and minimize pollution in chemical synthesis and processing. Heterogeneous catalysis is key to successful development of so-called "green chemistry" since it is widely used to reduce emissions from automobile and stationary combustion sources. For example, emission of CO from automobiles is substantially diminished by heterogeneous catalysts, such as oxide-supported platinum-group materials used in the three-way catalyst.[1−3] Heterogeneous catalysts are also essential for chemical production and processing in the petroleum industries.[4−6] Development of low-temperature processes would improve the selectivity of important chemical reactions, thus reducing the byproducts and energy consumption and potentially limiting production of chemicals that may be unfriendly to the environment or human health.

In this paper, we focus on the use of heterogeneous gold catalysts for low-temperature oxidative reactions. We also introduce the concept of using metastable phases of oxygen as a means of enhancing the activity and selectivity of catalysts in general and Au-based catalysts in specific.

The discovery that gold is active for heterogeneous oxidative reactions at low temperature—e.g., CO oxidation[7] and selective propene oxidation[8]—made by Haruta and colleagues motivated a considerable amount of research on the activity of gold-based catalysts. The importance of new processes for low-temperature CO oxidation, for example, is underscored by noting that current commercial catalysts for automotive pollution control, which are based on platinum-group metals, are not very active at low temperature, leading to the "cold start-up" problem in which much of the CO produced by incomplete combustion is not oxidized for operation temperatures below 200 °C.[1,9,10] Gold-based catalysts oxidize CO at much lower temperature (even at room temperature or below), although application of the gold catalysts in conjunction with the platinum-based three-way catalysts would require improvement in their thermal stability.[1,9−11]

The other area where gold catalysts have potential to enhance performance is in the selective epoxidation of propene and other olefins.[8,12] Propene epoxide is an important starting material in the chemical industry for the synthesis of polyether polyols, polyurethane, and propene glycol.[12,13] Existing commercial processes for producing propene epoxide are the chlorohydrin process and the hydroperoxide process (Halcon). In the chlorohydrin process, propene first reacts with hypochlorous acid to produce chlorohydrin followed by dehydrochlorination using aqueous potassium hydroxide to produce the epoxide. In the hydroperoxide process, the propene reacts with alkyl-hydroperoxides which are produced by the peroxidation of an alkane, resulting in propene oxide and alcohol as products. The details of those processes have recently been reviewed,[13] and both have serious drawbacks. The chlorohydrin process produces chlorinated byproducts which create an environmental hazard. The hydroperoxide process is expensive and also yields styrene and *tert*-butyl alcohol as coproducts.[13] Ideally, propene would be directly oxidized using oxygen with the aid of a heterogeneous catalyst. The primary obstacle to direct heterogeneous oxidation of propene to propene epoxide is that the allylic C−H bond in propene is very labile and subject to attack by oxygen. Silver catalysts, used for

* To whom correspondence should be addressed.
† Department of Chemistry and Chemical Biology, Harvard University.
‡ Current address: Hydrogen Energy Research Center, Korea Institute of Science and Technology, 39-1 Hawolgok-dong, Seongbuk-gu, Seoul, 136-791, Korea.
§ Division of Engineering and Applied Sciences, Harvard University.

10.1021/cr050954d CCC: $65.00
Published on Web 06/13/2007

Byoung Koun Min received his B.S. and M.S. degrees in 1996 and 1998, respectively, in the Department of Chemistry at Korea University in Seoul, Korea. In 1999 he went to the United States to begin his doctoral studies in the Department of Chemistry at Texas A&M University and received his Ph.D. degree in 2004 under the direction of Professor D. Wayne Goodman. He subsequently moved to the Department of Chemistry and Chemical Biology at Harvard University as a postdoctoral fellow and worked with Professor Cynthia M. Friend until August 2006. Afterward, he was appointed as a senior research scientist in the Hydrogen Energy Research Center of the Korea Institute of Science and Technology (KIST). His research interests during his Ph.D. and postdoctoral program have been centered around design and synthesis of model catalytic systems and their application to catalytic and surface reactions, particularly related to gold catalysts. On the basis of these studies, 25 research papers have been published in international peer-reviewed journals. His current research is focused on more applicable interests such as hydrogen energy and solar cells.

Professor Cynthia Friend is widely known for her leading research on surfaces and interfaces with expertise in heterogeneous catalysis, nanoscience, heterogeneous environmental chemistry, electronic and optical materials, adhesion and wear properties, and energy technologies. She began her academic career in the Chemistry Department at Harvard University in 1982 after completing her Ph.D. degree in Chemistry at the University of California in 1981 and a year of postdoctoral research at Stanford University. Her work has been recognized by a number of national awards, including the Garvan Medal of the American Chemical Society. In recognition of her research and teaching accomplishments, she was appointed as the Morris Kahn Associate Professor in the Faculty of Arts and Sciences in 1988 and promoted to the rank of Professor of Chemistry in 1989. In 1998, she was named the Theodore Williams Richards Professor of Chemistry in the Department of Chemistry and Chemical Biology (CCB), and in 2002 she was appointed as Professor of Materials Science in the School of Engineering and Applied Sciences. She is carrying out numerous leadership roles within the Harvard community. She is the first female Chair of CCB. Since 2002, she has served as Associate Director of the Materials Research Science and Engineering Center (MRSEC). She also served as Associate Dean of the Faculty of Arts and Sciences between 2002 and 2005. She also serves on the Executive Committees of the Harvard Nanoscale Science and Engineering Center (NSEC) and Center for Imaging and Mesoscale Systems (CIMS).

commercial epoxidation of ethylene, lead to combustion of propene *not* epoxidation because of the activation at the allylic proton, for example. On the other hand, recent studies of gold catalysts indicate that they may be commercially viable for propene epoxidation.[14,15]

In this paper, we review the current understanding of the important features of gold catalysts for low-temperature CO oxidation and propene oxidation with a focus on fundamental aspects obtained from surface science studies. In the first part of this paper, we briefly provide an overview of previous investigations of high surface area and model catalysts and related theoretical studies. Subsequently, we highlight some of our work using oxidized Au(111) that is relevant to the fundamental underpinnings of gold catalysis. In particular, we introduce the concept of using metastable oxygen species to promote selective oxidation reactions. Metastable oxygen on Au(111) has a high activity and selectivity toward both CO and propene oxidation. Our studies suggest that metastable oxygen species may be useful in a broad range of reactions on Au. Under reaction conditions, metastable oxygen phases can, in principle, be created by selecting appropriate reaction conditions that kinetically control the state of the surface. Control of the temperature and pressures (flux) of reactants will affect the state of the surface, even for high surface area materials.

2. Overview of Heterogeneous Gold-Based Catalysis

2.1. Low-Temperature CO Oxidation

The discovery that small, nanoscopic gold particles supported on metal oxides are active for low-temperature CO oxidation has inspired a considerable amount of research directed toward understanding the basis for the activity of Au catalysts. Interestingly, the activities for CO oxidation for high surface area gold catalysts[11,16,17] and a model system with Au supported on a planar oxide support[18,19] are similarly sensitive to the gold particle size distribution (Figure 1).

Even though, as mentioned, it has been generally agreed that the catalytic activity of gold depends on the size of the gold particles, the underlying physical explanation for the activity of gold has been the subject of extreme controversy. The complexity of the gold catalytic system introduces many possible factors that can contribute to the catalytic activity of gold. Both the metal oxide and the Au itself may be important in determining the activity. In particular, edge sites and electronic perturbation of the Au due to its interaction with the support have been suggested to be important for activity. In addition, the presence of moisture, present in many high-pressure reaction systems, seems to promote activity of Au for CO oxidation.

Here, we classify the possible contributions to the activity of Au into two broad categories: factors related to the gold particle itself and factors related to the oxide support as outlined in Scheme 1. The size, thickness, or shape of the gold particles all fall in the first category, and the oxide support is considered a passive supporting material, the primary role being to provide sites for the nucleation and growth of gold nanoparticles. One of the primary explanations for gold activity for CO oxidation is that there are undercoordinated gold atoms, the prevalence of which is related to the size, thickness, or shape of the gold particles.

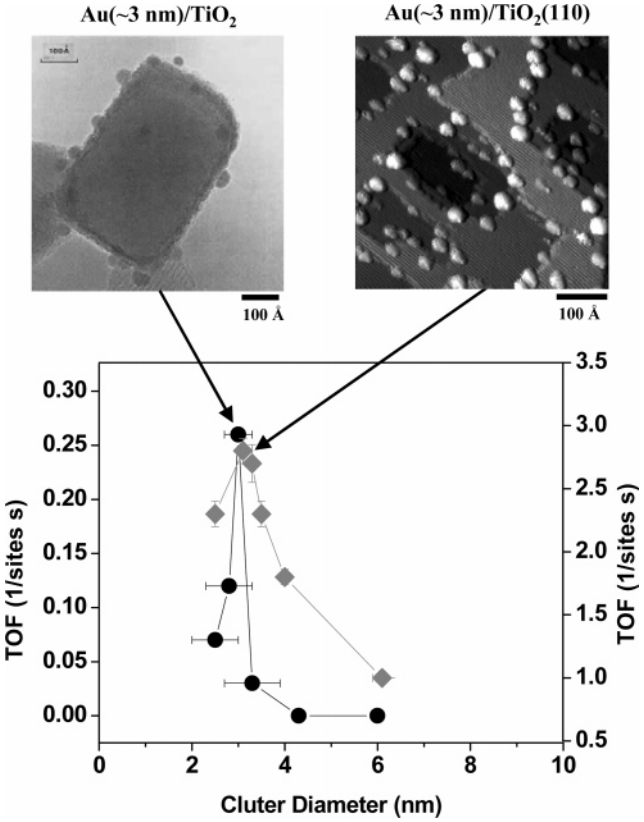

Figure 1. Transmission electron micrograph of Au (3.3%) supported on TiO_2 prepared by deposition−precipitation method (left), and STM image (right) of Au/TiO_2 (110) prepared by physical vapor deposition method in UHV conditions. The average gold particle size in both cases is ∼3 nm. The reactivity data (turnover frequencies, TOFs) of gold catalysts in CO oxidation at 300 K as a function of the average size of gold particles supported on the high surface area catalysts and TiO_2 (110)-(1 × 1). The right transmission electron micrograph and the plot of TOF versus cluster diameter are reprinted with permission from ref 18 (www.sciencemag.org). Copyright 1998 AAAS. The left transmission electron micrograph is reprinted from ref 137, Copyright 1993, with permission from Elsevier.

In the second category, the oxide support is thought to contribute to the catalytic activity of Au through several mechanisms: (1) charge transfer to/from the oxide support from/to the gold particle, (2) supply of adsorption sites for reactants, in particular, oxidants, that may migrate to the Au particle, and (3) formation of a reactive gold−oxide interface and the particle perimeter. In this section, we briefly review previous studies that address these various points for Au-induced CO oxidation.

2.1.1. Influence of the Characteristics of Gold Particles on CO Oxidation Activity

A natural question about the influence of the characteristics of Au particles on CO oxidation is whether Au that is *not* supported on oxide materials is active for CO oxidation. Indeed, unsupported gold powder is active for CO oxidation between 249 and 294 K when a closed recirculation reaction system is used,[20] albeit the rate constant is lower by 2 orders of magnitude for the Au powder compared to gold nanoparticles supported on titania after accounting for the surface area of the gold. The diameters of the Au particles (mean diameter of 3.5 nm) supported on TiO_2 were smaller than the unsupported powder, which had a mean diameter of 76 nm. Thus, it is not clear whether the difference in reactivity

Scheme 1

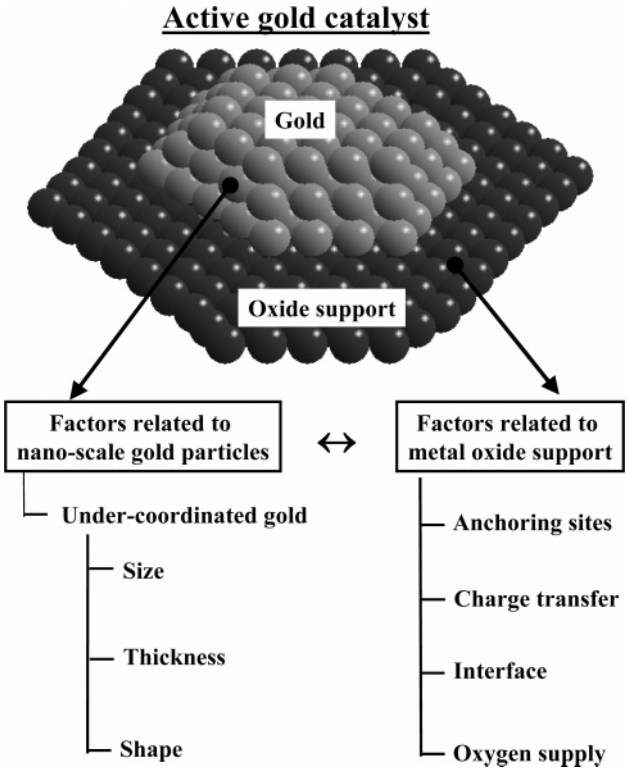

for the supported and unsupported Au is due to the support or a difference in the gold particle size distribution.

Studies of CO oxidation on supported Au nanoparticles definitively show that smaller particles are more active on a variety of oxide supports. Specifically, small gold particles (2−4 nm in diameter) have an activity at 273 K that is more than 2 orders of magnitude larger than larger gold particles (20−40 nm in diameter) irrespective of whether those are supported on a reducible or an irreducible oxide.[21] These results strongly indicate that Au particle size has a major effect on activity for CO oxidation. Although the particle size is clearly an important factor in determining reactivity, the shape of the particles and, therefore, the coordination sites available are also important. The shape of the particles in turn depends on the metal oxide support. For example, a recent study was performed on gold particles having almost identical size distributions (∼3 nm) prepared on different oxide supports using the colloidal deposition method.[22] The differences in the measured rates of CO oxidation for different supports were attributed to differences in the shapes of the Au particles on the various oxide supports since the activities reported did not follow the trend reported by others. Specifically, gold particles supported on alumina, which was reported to be inactive by others,[21,23] are more active than those supported on the reducible oxides similar to ZnO.[23]

Clearly, small gold particles in a variety of environments are active for CO oxidation, even without a support. This observation raises the question as to why small-sized gold is active whereas extended Au surfaces, e.g., single crystals, are not. Notably, CO is readily oxidized on extended Au surfaces once oxygen atoms are present on the surface, as discussed in more detail below; however, there is not a successful example of extended Au surfaces being catalytic.

Early on it was suggested that the catalytic activity of Au is due to different electronic properties associated with Au nanoparticles supported on metal oxides. The onset of

catalytic activity of small gold particles supported on TiO_2(110) correlated with a metal-to-nonmetal transition that was suggested by scanning tunneling microscopy (STM) and spectroscopy (STS) measurements.[18] Specifically, the band gaps of one-atom-thick gold particles measured by STS were significantly larger than the gap measured for two-atom-thick gold particles, which had band gaps in the range of 0.2−0.6 V. Larger particles with a thickness of three atoms or more were metallic in STS. The proposal that the *thickness* of the gold is important was reinforced by the same group based on studies of well-ordered monolayer and bilayer films of Au on a Ti_2O_3 thin film grown on Mo(112). The activity for CO oxidation at 5 Torr was more than an order of magnitude higher for the gold bilayer compared to a one-layer-thick film, indicating that the thickness of gold particles is important.[24]

However, there is controversy regarding the explanation of activity based on electronic factors due to quantum size effects, such as layer thickness. For example, in one model system, gold particles with various sizes and thickness were deposited on FeO(111) films, and CO adsorption was found to be essentially independent of particle thickness since the relative intensities of CO desorption peaks increase with increasing gold coverage, not showing unique CO adsorption behavior with respect to the thickness of gold particles.[25] This result is at odds with trends in the isosteric heats of adsorption ($-\Delta H_{ads}$) for CO measured on gold particles supported on TiO_2(110), which depended strongly on the Au cluster size—the highest $-\Delta H_{ads}$ correlates strongly with the system exhibiting the maximum activity for CO oxidation in the Au/TiO_2(110) system.[26] Furthermore, CO oxidation to CO_2 was found to be only weakly dependent on the particle size when Au particles supported on TiO_2 were oxidized by a supersonic beam of oxygen atoms. In this case, CO reacts with adsorbed oxygen adatoms at 77 K.[27] These results suggest that the particle size of Au is important in supplying oxygen—in particular, atomic oxygen—to CO, not in determining the binding of CO itself.

An alternative explanation of the origin of the catalytic activity of small gold particles is the presence of undercoordinated Au atoms, possibly as sites for binding or dissociation of O_2.[21,28−30] Theoretical calculations of the structures of small Au particles supported on TiO_2 predict that there are a significant number of undercoordinated gold atoms.[31] As would be anticipated, the step density—defined as the fraction of atoms in the particle having seven or less neighbors—increases continuously as the particle size decreases (Figure 2). The theoretical calculations indicate that gold particles that are bilayers maximize undercoordinated gold sites for a given particle size, which suggests that the effect of thickness proposed previously was really a proxy for the presence of a large fraction of undercoordinated sites in small gold particles. The importance of undercoordinated gold sites is further elucidated by the fact that calculated adsorption energies for both CO and O atoms depend strongly on the Au coordination number.[21] The theoretical results (Figure 3) show that the strength of Au−CO and Au−O varies strongly with the gold coordination number, and both the O and CO adsorption energies are lowered (stronger bonding) by up to 1 eV going from Au(111) (coordination number 9) to the Au_{10} cluster (coordination number 4).

The theoretical calculations in this case assume that CO is oxidized by reaction with atomically adsorbed oxygen in

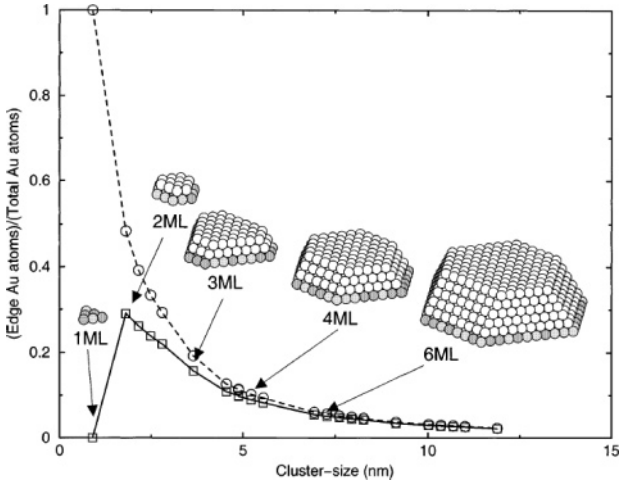

Figure 2. Calculated step density for Au particles on TiO_2 as a function of particle size. (○ and □) Total and "free" step sites on the Au particles. "Free" are the step sites not in direct contact with the support. Lines through the two sets of points are only drawn as a guide to the eye. Insets illustrate the corresponding Wulff constructions for selected particle sizes. Reprinted from ref 31, Copyright 2000, with kind permission of Springer Science and Business Media.

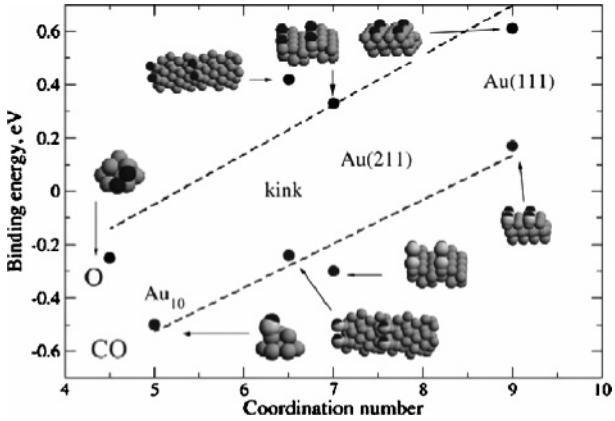

Figure 3. Correlation between the binding energies, for CO molecules and O atoms, with respect to the coordination number of Au atoms in a series of environments. Binding energies, in eV, reported are referred to gas-phase CO and O_2; for O_2 the energies are given per O atom. Reprinted from ref 21, Copyright 2004, with permission from Elsevier.

a Langmuir−Hinshelwood mechanism. The Langmuir−Hinshelwood model has been applied to describe the CO oxidation mechanism occurring on platinum-group metals, and it has been confirmed by a number of UHV studies and steady-state kinetics.[32−35] In the Langmuir−Hinshelwood model, CO oxidation occurs on the surface in the following steps

$$CO(g) \rightarrow CO_{ads} \quad (1)$$

$$O_2(g) \rightarrow 2O_{ads} \quad (2)$$

$$CO_{ads} + O_{ads} \rightarrow CO_2(g) \quad (3)$$

Depending on the properties of metals (e.g., metal−oxygen bond energies), the rate-determining step of this reaction may be different. For example, if the metal (e.g., Ru) can form stable oxides (high M−O bond energy), the rate-determining step will be the reaction between CO_{ads} and O_{ads}, whereas for a metal (e.g., Ag) that has a lower M−O bond energy,

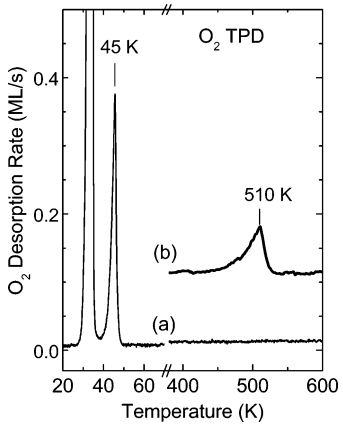

Figure 4. Temperature-programmed desorption spectra of O_2 from (a) a 10 ML thick O_2 film deposited on the Au substrate and (b) 1 ML of atomic Au deposited on 10 ML of O_2 at 22 K. Reprinted with permission from ref 39. Copyright 2005 American Chemical Society.

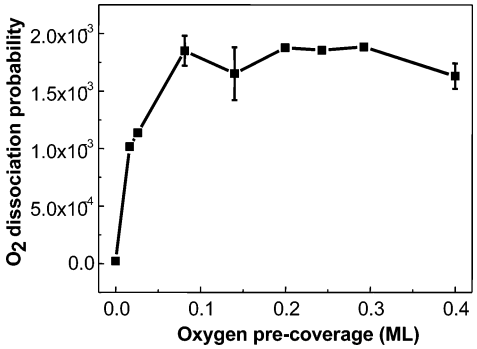

Figure 5. Sticking probability of $^{18}O_2$ on Au(111) as a function of oxygen precoverage. The oxygen precovered Au(111) was prepared via electron bombardment of condensed NO_2, and $^{18}O_2$ was dosed using background dosing with a pressure of 1×10^{-7} Torr for 1 min for all experiments. The sticking probability is estimated from temperature-programmed desorption experiments. Reprinted with permission from ref 41. Copyright 2005 American Chemical Society.

the rate-determining step will be adsorption or dissociation of molecular oxygen on the metal surface.[36]

By analogy to the platinum-group metals, gold is expected to follow the Langmuir−Hinshelwood model for CO oxidation, which means that CO is adsorbed (1) on the gold surface, oxygen dissociates (2), and the adsorbed CO and oxygen react to form CO_2 (3), which leaves the surface. However, different from other metals, extended gold surfaces are not active for this process, primarily because O_2 does not readily dissociate on the surface. Furthermore, CO is weakly bound on gold single-crystal surfaces only remaining on the surface at very low temperature, e.g., below 140 K for Au(110),[37] leading to a short surface lifetime for CO bound to Au near room temperature. Even for the supported gold particles, CO is weakly adsorbed compared to Pt-group metals, desorbing below 200 K in UHV conditions from Au supported on TiO_2 which has undercoordinated gold.[25] Nevertheless, low-temperature oxidation of CO does, indeed, occur on both extended Au surfaces and Au particles when atomic oxygen is present.

The limiting factor in CO oxidation on extended surfaces is the low rate of O_2 dissociation. For example, oxygen does not dissociate to any measurable degree even at high-temperature (500 K) and high-pressure conditions (1400 Torr) on clean Au(110).[38] In fact, O_2 itself is weakly adsorbed on extended Au, desorbing below 50 K (see Figure 4).[39] Adsorption of O_2 after exposure of gold to pressures of O_2 in the range of 3−6 Torr at 200 °C has been traditionally used to measure gold surface area;[38] however, adsorption has been associated with the presence of impurities, such as Ca or Si, which promote oxygen adsorption on Au.[40]

While all evidence indicates that O_2 dissociation does not occur on extended Au surfaces, two recent studies provide evidence that undercoordinated gold sites can facilitate oxygen dissociation even on extended gold surfaces. As expected, there is no measurable dissociation of O_2 on Au(111) under UHV conditions, establishing an upper limit on the dissociation probability of 10^{-7}.[41] Nevertheless, creation of undercoordinated Au atoms on Au(111) does lead to measurable O_2 dissociation at 400 K (Figure 5). Undercoordinated Au atoms were created on Au(111) by deposition of oxygen atoms via electron-induced dissociation of NO_2. Once some oxygen is deposited, the O_2 dissociation probability was measured to be 10^{-3} (Figure 5). This enhancement of O_2 dissociation was attributed to formation of a rough surface due to preadsorption of atomic oxygen, leading to creation of undercoordinated gold sites, which may be responsible for O_2 dissociation.[42] The roughening of the surface was established using scanning tunneling microscopy. As discussed below, the degree of surface roughening depends on the oxidation conditions. In an independent study, O_2 dissociation induced by Au was also observed at cryogenic temperatures.[39] In this case, multilayers of O_2 (10 ML thick) were condensed on a thick Au film at 22 K, and Au atoms were subsequently deposited onto this surface. Evidence for O_2 dissociation induced by the Au atoms impinging on the surface is based on the observation of an O_2 peak characteristic of oxygen-atom recombination at 510 K in temperature-programmed desorption as well as peaks due to sublimation of condensed O_2 at 35 K and desorption of molecular O_2 at 45 K (Figure 4). Both of these studies indicate that undercoordinated Au atoms can induce O_2 dissociation even if they are supported on bulk Au.

Once atomic oxygen forms on gold—whether it be extended gold surfaces or small particles—CO oxidation readily occurs at low temperature.[39,43−46] Indeed, CO oxidation to CO_2 even occurs at a temperature as low as 35 K, as long as atomic oxygen is present,[39] implying that the activation barrier of the reaction between CO and O is extremely low. More details of CO oxidation studies using an oxidized gold single crystal will be addressed in the following section.

It is also interesting to note that supported gold particles are exposed to oxygen during catalyst preparation (e.g., drying or calcination) and that the pretreatment conditions affect the CO oxidation activity of supported Au.[47] The rates of CO oxidation at 303 K over Au/TiO_2 catalyst are higher for the oxidizing pretreatment, in comparison to pretreatment in either an inert or reducing environment. More importantly, it was also found that the gold phase which was characterized by XPS and X-ray absorption fine structure (XAFS) is changed from an oxidized phase to a metallic one as the calcination temperature increases, and a higher reaction rate was observed in oxidized gold.

The increase in CO oxidation rate for high surface area catalysts that are oxidized during calcination or drying (most probably to a Au_2O_3-like phase) suggests that positively charged gold might be more active for CO oxidation than Au^0. In order to address this issue, a MgO-supported Au(III)

complex whose oxidation states can be varied using different reducing conditions (i.e., various CO partial pressures in the reaction mixture) were used and the reaction rate was measured as a function of the surface concentration of positively charged gold (Au^+) or metallic gold (Au^0).[48,49] Each oxidation state of the catalyst was characterized by extended X-ray absorption fine structure (EXAFS) and X-ray absorption near-edge structure (XANES) subsequently. Higher concentrations of positively charged gold (corresponding to lower partial pressure of CO in the reaction mixture) lead to higher catalytic activity, suggesting that the simultaneous presence of metallic gold atoms adjacent to cationic gold is crucial in the catalytic activity of gold.

2.1.2. Factors Related to the Oxide Support

Anchoring Sites for Gold Particles. Even though metallic Au is active for CO oxidation, the oxide support does play a role. Obviously, the oxide support provides sites for anchoring gold particles so as to maximize surface area (and, therefore, the fraction of undercoordinated Au atoms). The support may also affect the dispersion and shape of the Au particles. The presence of defects on oxide surfaces is known to provide sites for nucleation and growth of metal particles, including Au.[50−57] As a first example, the role of oxygen vacancies on TiO_2(110) in the nucleation and growth of gold particles was clearly demonstrated by STM studies.[50] By measuring the number density of oxygen vacancies and gold particles which are distinguishable in the contrast of STM images it was found that the density of oxygen vacancies on TiO_2(110) decreases during gold particle growth (Figure 6). Theoretical results also support this experimental observation by showing that the adsorption energy of a single gold atom on an oxygen vacancy site is more stable by 0.45 eV than on the stoichiometric surface.[50] The nucleation and growth features of gold particles on TiO_2(110) are often changed depending on the density of oxygen vacancies on the terrace, which is usually influenced by sample preparation conditions. In some cases where the density of oxygen vacancies on terraces is low, gold particles preferentially nucleate and grow on the extended defects such as step edges of the oxide surfaces, as can be seen in Figure 1.[54,57]

Similar to the TiO_2(110) surface, gold particles were found to preferentially nucleate and grow on defect sites such as

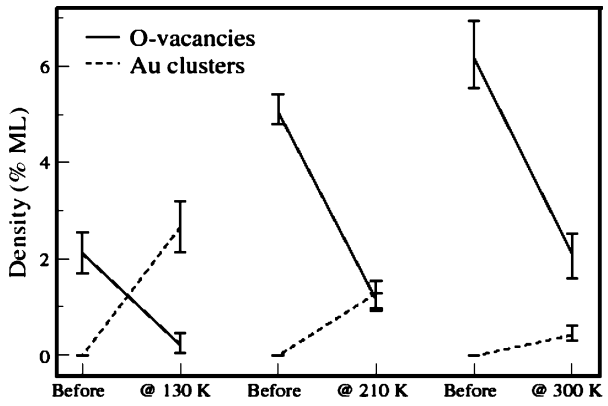

Figure 6. Densities of vacancies and Au clusters before and after deposition of ~0.04 ML Au at different temperatures. 1 ML = 1 vacancy or cluster/TiO_2 (110) unit cell = 5.13×10^{14} cm^{-2}. The data were obtained from corresponding high-resolution STM images. Reprinted with permission from ref 50 (http://link.aps.org/abstract/PRL/v90/p026101). Copyright 2003 by the American Physical Society.

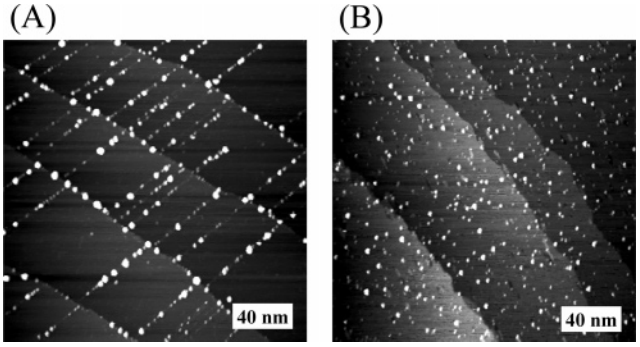

Figure 7. STM images (200 nm × 200 nm) of gold particles supported on a SiO_2 thin film annealed at (A) 1200 (less defective) and (B) 1100 K (more defective). In the film A, gold particles nucleate and grow preferentially at step edges and line defects, while more random distributions of gold particles on terrace regions were observed in the film (B). Reprinted with permission from refs 52 and 53. Copyright 2004 American Chemical Society.

step edges and/or line defects of a well-ordered SiO_2 thin film grown on a Mo(112) single crystal at room temperature (Figure 7A).[51−53] Defective SiO_2 surfaces, where the oxygen vacancies are predominantly on terraces, nucleate gold particles on the terrace area with higher density than less defective SiO_2 films (Figure 7B). The importance of nucleation and growth of gold particles at defect sites was also observed in Al_2O_3 and FeO thin films at room temperature, confirming that defects are the active sites for anchoring gold particles.[58] The primary effect of defect-mediated nucleation and growth is to favor growth of small particles that are relatively strongly bound to the support and thus more resistant to agglomeration.

Negatively Charged Gold Particles. In addition to the role of the oxide support for anchoring gold particles, many studies have pointed out that defect sites (e.g., oxygen vacancies) might play an important role in charge transfer to gold particles, resulting in formation of *negatively* charged gold particles which can enhance the catalytic activity for CO oxidation.[24,59−63] This assertion is diametrically opposite to proposals that positively charged Au is most active. These differences may be due to differences in model vs realistic catalysts which are prepared very differently (e.g., calcinations or drying procedure in the preparation of high surface area catalysts, not in model catalysts). The study of low-temperature CO oxidation using gold octamers (Au_8) supported on MgO (001) showed that gold octamers bound to a MgO surface rich in oxygen vacancies (F centers) can catalyze CO oxidation, whereas gold particles deposited on MgO surfaces nearly free of oxygen vacancies are catalytically inactive.[59] This phenomenon was attributed to partial electron transfer from the F center to the gold particles, which in turn promotes activation of adsorbed reactant molecules according to both experimental and theoretical investigations. The frequency of the C≡O stretch of adsorbed CO shifts to lower frequency by about 25−50 cm^{-1}, resulting from the back-donation of charge from the gold particles to the antibonding $2\pi^*$ orbital of the CO adsorbed on the gold particle anchored to the F center of the surface.

The importance of negatively charged gold in catalytic activity was also emphasized in the model study using gold film grown on a Ti_2O_3 thin film which was synthesized on Mo(112).[24,61,62] The CO stretch energy for CO bound to this gold film is 2088 cm^{-1}, which is closer to that observed on gold single crystals than to positively charged gold where Au is bonded to Ti via oxygen. This observation suggests

that Au directly bonds to Ti, which is analogous to gold bonded to oxygen vacancies of the TiO_2 surface. Furthermore, the high-resolution electron energy loss spectroscopy (HREELS) data indicated a $Ti^{4+}-O$ vibrational feature on the gold film covered Ti_2O_3 surface, which again supports formation of negatively charged Au due to the charge transfer from Ti^{3+} to Au. The catalytically active electron-rich gold thin film (monolayer) was further confirmed by infrared spectroscopic studies, showing the shift of the CO vibrational frequency to lower compared to the bulk-like gold film.[62]

The charge transfer from oxygen vacancies of $TiO_2(110)$ to gold particles was more directly investigated using photoelectron spectroscopy (PES).[63] The PES results show that the O(2p) nonbonding peak shifts to lower binding energy accompanied by the disappearance of the Ti(3d) peak due to the deposition of gold particles on the $TiO_2(110)$ surface. Since the O(2p) nonbonding peak of the reduced TiO_2 appears at higher binding energy due to band bending associated with extra electrons originating from surface defects, a red shift of the O(2p) nonbonding peak and disappearance of the Ti(3d) peak observed in gold deposited onto the TiO_2 indicates loss of extra electrons due to charge transfer to gold particles.

The importance of negatively charged Au in reactivity was also emphasized in several theoretical studies[50,64−67] and gas-phase studies of Au_n^- anion cluster with oxygen.[68−70] Particularly, good agreement in gas-phase studies has been made in the reactivity behavior of odd−even number of gold atoms for less than 20 Au. The even-numbered anion gold clusters adsorb O_2 and are, therefore, suggested to be active for CO oxidation, although there has not been a direct measurement of activity for the reaction, whereas odd-numbered anion gold clusters do not show reactivity toward O_2 adsorption. This phenomenon was explained by the fact that the even-numbered anion gold clusters have an odd number of electrons which enables donating one electron to the adsorbed O_2 molecule in order to achieve the closed shells/subshells.[70]

Clearly, there is controversy regarding the degree and direction of charge transfer to/from the Au particles supported on TiO_2. Apparently, both negatively and positively charged particles can play a role in CO oxidation, although their specific roles are not clearly defined.

Interface and Moisture Effects. The role of interface sites between gold particles and the oxide support has been regarded as adsorption and reaction sites for CO oxidation. This was proposed for the first time by Haruta et al. using high surface area gold catalysts, based on their IR absorption data where two distinct CO vibrational features were observed.[11] They assigned the CO vibration peak at higher frequency to a linearly bonded carbonyl on gold particles, while the lower frequency one was assigned to CO adsorbed on the interface perimeter. Dissociation of molecular oxygen at the interface was also suggested in a study using Au supported on Fe_2O_3.[23] On the basis of $CO-O_2$ titration experiments, it was claimed that a significant amount of molecular oxygen can adsorb on the Fe_2O_3 support and that this oxygen readily migrates to the interface followed by subsequent reaction with CO. Atomic oxygen formation under these reaction conditions was detected by diffuse reflectance infrared Fourier transform spectroscopy (DRIFTS), indicating that dissociation of molecular oxygen occurs at the interface.[71] A similar picture of the role of the interface and related CO oxidation mechanisms was also suggested by studies using various model systems including Au supported on TiO_2 powders and thin films.[72]

Several theoretical studies have shown that O_2 can adsorb at the interface between the gold particle and the oxide support and that the reaction barrier for CO oxidation is very low (0.1−0.4 eV) at the interface.[28,73−77] For example, the energetics of CO oxidation were calculated using three different Au−MgO interface boundaries with respect to gold particle size and gold/oxide contact structure (degree of wetting).[76] Excluding the possibility of O_2 dissociation due to a high calculated energy barrier (~1 eV), a pathway where an adsorbed $CO-O_2$ reaction intermediate exists in the interfacial region is energetically favorable. Furthermore, the results imply that the gold particle which has a nearly hemispherical shape would have a very low energy barrier for CO_2 formation.

The adsorption energy and reaction barrier were also calculated for CO oxidation on $Au/TiO_2(110)$ and non-supported Au using density functional theory (DFT).[77] Three important points were derived from these studies: (i) CO adsorption on Au is quite strong (1.7 eV) irrespective of the presence of the oxide for models containing two layers of Au, (ii) O_2 can be dissociated with a low barrier (0.52 eV) at the Au/TiO_2 interface (however, O_2 dissociation is not favorable on unsupported Au ($E_a > 2$ eV)), and (iii) CO oxidation via a $CO-O_2$ complex has a relatively low barrier (0.1 eV) at the Au/TiO_2 interface but a higher barrier for the unsupported Au.

Even though many studies (e.g., especially theoretical studies) suggested that the gold−oxide support interface plays a role as an O_2 adsorption and reaction site, one question arises how the limited interface area of the gold catalytic system can be responsible for O_2 adsorption prior to reaction with CO.[78] Several groups conclude that the perimeter of the Au particles is not sufficient to adequately supply oxygen for reaction and that water adsorbed on the metal oxide support somehow facilitates transfer of oxygen to the support.[47,78−82] The CO oxidation rate at 270 K over Au/TiO_2 catalysts increases when water is present, up to 200 ppm H_2O. At higher humidity, the rate falls.[80] Importantly, the difference in the rate between 0.1 (a highly dried condition) and 3 ppm (a typical reaction condition) is one order magnitude, indicating a strong influence of moisture. More recently, the role of moisture in CO oxidation was further examined using three different gold catalysts supported on TiO_2, Al_2O_3, and SiO_2 (gold particle size is 3.0, 3.9, and 8.2 nm in mean diameter, respectively).[79] Even though there are some variations in the activity profile depending on the support material, there is a general increase in activity with respect to the moisture content over a wide range of concentration from 0.1 to 6000 ppm H_2O.

It is important to note that the effect of moisture on CO oxidation is strongly correlated with the role of the oxide support because the oxide support serves as a moisture reservoir. This aspect was addressed in a recent theoretical work,[78] and several important points were made: (i) water can dissociate to form hydroxyl species at oxygen vacancies of $TiO_2(110)$ surface, (ii) these hydroxyl species stabilize O_2 adsorption, and (iii) O_2 can diffuse along the channel of Ti (five-coordinated) atoms on $TiO_2(110)$ to the Au/TiO_2 interface. It was suggested that the origin of O_2 adsorption on the TiO_2 surface in the presence of hydroxyl species is charge transfer from TiO_2 to O_2 due to the reduction by H atoms created by water dissociation.

Another recent theoretical study[81] of gold particles supported on defect-free MgO surface, which avoids charging due to electron transfer from defect sites of the oxide support, reported a larger adsorption energy for the coadsorption of H_2O and O_2 than those for two individual species, indicating a synergic effect between H_2O and O_2. The optimized coadsorption configuration indicates a hydroperoxyl-like intermediate accompanied by partial charging of the O_2 molecule from H_2O, resulting in activation of the O−O bond and consequently reaction with CO with a small activation barrier of ~0.5 eV.

In brief, in addition to the primary role of the oxide support for providing anchor sites for gold particles, the oxide support—particularly defects and interface sites— plays a crucial role in the enhancement of catalytic activity of gold in CO oxidation as a provider of extra charge to gold particles or oxygen to proximity of gold. The former may be related to more direct activation of molecular oxygen by gold because electron-rich gold is expected to result in either increased binding of molecular oxygen to the gold surface or facile activation of molecular oxygen (i.e., O−O bond breaking or formation of peroxo or superoxo species) since more charge can be transferred to the antibonding $2\pi^*$ orbital of O_2, whereas the latter is associated with indirect activation of molecular oxygen through interaction with moisture present on the surface where hydroxyl species from moisture may either stabilize O_2 adsorption or assist charge transfer to the O_2 to be activated.

2.1.3. Active Oxygen Species (Atomic or Molecular)

Although it is clear that CO adsorbs on gold, even if weakly,[83,84] and that atomic oxygen adsorbed on Au rapidly reacts with CO to form CO_2,[39,43−46] there is still debate regarding the nature of the active oxygen intermediate in CO oxidation.[78,81,85] The debate regarding the oxygen intermediate arises from the fact that the dissociation probability for O_2 on extended Au surfaces and Au nanoparticles supported on TiO_2 is very low, $\leq 10^{-7}$.[41] Accordingly, molecular oxygen, i.e., a peroxo species, has been proposed to be the active oxygen species for CO oxidation by some.[81,86,87] On the other hand, there is evidence for O_2 dissociation when undercoordinated gold atoms are present on extended Au surfaces under model conditions.[39,41]

The possibility that both atomic and molecular oxygen are active for CO oxidation has been studied theoretically. Theoretical studies have specifically considered the effect of Au−Au bond expansion and the presence of steps on the activation barrier for O_2 dissociation using DFT calculations. The activation energies for O_2 dissociation depend strongly on the coordination number and lattice constant in Au, as illustrated by the fact that the barriers calculated for 10%-stretched Au(111), unstretched Au(211), and 10%-stretched Au(211) are 1.37, 1.12, and 0.63 eV, respectively.[88] These results suggest that small gold particles supported on metal oxides should have a lower barrier for O_2 dissociation because of the higher concentration of steps expected in smaller gold particles[31] and the lattice strain of gold particles induced by an oxide support.[89] On the other hand, there is no direct experimental evidence for stretched Au−Au bonds in nanoclusters. Other DFT calculations find that the lowest activation barrier for oxygen dissociation ($E_a = 0.93$ eV) is at the step site on Au(211), which is too high to induce O_2 dissociation at room temperature based on a rough estimation of the initial sticking coefficient ($S_o \approx 10^{-21}$) of O_2 on Au steps.[90]

An alternative model for CO oxidation is direct reaction with molecular oxygen. Indeed, there is experimental evidence that the η^1-superoxide and peroxide react with CO on gold particles supported on nanocrystalline CeO_{2-x} based on a comparison of O_2 adsorption features in Raman spectra before and after CO exposure.[87] Formation of an asymmetric four-center O−O−CO metastable intermediate on Au steps has been suggested based on theoretical studies.[90] This intermediate is proposed to decompose to CO_2 and adsorbed O. The remaining oxygen atoms would react with a second CO to yield CO_2. There is a small barrier for formation of the asymmetric O−O−CO intermediate, ~0.46 eV. Similarly, formation of a carbonate intermediate from reaction of CO with molecular oxygen on Au_2^- has also been proposed based on DFT calculations.[91]

The role of water in facilitating CO oxidation is also important in considering the mechanism for CO oxidation. One proposal is that H_2O imparts a partial negative charge to O_2 through population of the antibonding molecular orbital, resulting in activation of the O−O bond by forming a hydroperoxy-like intermediate, whose length extends to values characteristic of superoxo- or peroxo-like states.[81] The calculated barrier for reaction of the O_2-H_2O complex with gaseous CO is 0.5 eV.

On the basis of the existing experimental and theoretical evidence, both atomic and molecular oxygen may contribute to CO oxidation activity on Au. The rate of CO oxidation by atomic oxygen is clearly most rapid; however, dissociation of O_2 is rate limiting. The rate of formation of atomic oxygen can be facilitated by formation of undercoordinated Au atoms. Alternatively, molecular oxygen might react with CO to form both CO_2 and adsorbed oxygen atoms that will subsequently react. The mechanism and active species for CO oxidation most likely depends on the nature of the Au species present and the reaction conditions (pressure and temperature).

2.2. Propene Oxidation

2.2.1. Overview

Interest in partial oxidation of propene using Au-based catalysts was ignited by the discovery of selective epoxidation of propene by gold catalysts reported by Haruta et al. in 1998.[8] Oxidation of propene by gold has many of the same issues as CO oxidation, but with the added complexity of the molecule, there are more reaction pathways to consider (Table 1). The most selective catalyst consists of gold particles supported on Ti-containing oxide supports—TiO_2 (anatase) and TiO_2–SiO_2—over which propene is oxidized to propene oxide (epoxide) with >90% selectivity in the presence of both hydrogen and oxygen.[8,12]

The selectivity for propene oxidation depends strongly on the nature of the metal oxide support, which could be due to the same set of factors enumerated for CO oxidation. For example, gold particles supported on Fe_2O_3 have a low activity for selective propene oxidation and combustion predominates.[12,92] In contrast, Au particles supported on irreducible oxides, e.g., SiO_2, MgO, and MoO_2, yield propanal, acetone, and acrolein with some C_2 oxygenates (ethanal and acetic acid).[92] It is also important to note that some partial oxidation of propene has been reported for metal oxide supports, such as Ti- and Al-containing hexagonal mesoporous silicas (HMS), Ti-modified high silica zeolite, titanium silicalite, and TiO_2(110), in the *absence* of gold particles.[93−95]

Table 1. Partial Oxidation of Propene on Gold Catalysts

catalyst	oxidant/reductant	product	selectivity (%)	remarks	ref
Au/SiO_2	O_2	acrolein	33		133
		acetone	3.5		
	$O_2 + H_2$	ethanal	~75	@ 200 °C	134
		propanal	~15		
		acrolein	~10		
	H_2 or D_2	propane			135
Au/TiO_2	$O_2 + H_2$	propene oxide	> 90		12
		propene oxide	67	<150 °C	134
		ethanal	~15	@ 200 °C	
		propanal	~30		
		propane	99 (plus any CO_2)		136
Au/MgO	$O_2 + H_2$	ethanal	~65	@ 200 °C	134
		propanal	~20		
		propene oxide	~20		
	H_2 or D_2	propane			135
Au(111)	O	acrolein	~53	further react to form acrylic acid and carbon suboxide	113

A recent review of Au-based propene oxidation highlights several important points.[12] First, both H_2 and O_2 are necessary for highly selective epoxidation of propene (>90%). As for CO oxidation, only small, supported gold nanoparticles—less than 5 nm in diameter[96]—efficiently promote epoxidation of propene. The method used for catalyst preparation is also important with catalysts prepared using the deposition−precipitation (DP) method, exhibiting high selectivity for epoxidation, whereas those synthesized using the impregnation method promotes combustion to CO_2 and H_2O. This difference is attributed to different contact structures of gold particles with the oxide support for the two methods. As noted above, selective oxidation is only observed when either the anatase phase of TiO_2 or titanosilicate (TiO_2–SiO_2) supports are used. Finally, conversion of propene to the epoxide is improved by up to 10% by alkaline and alkaline earth salts used as promoters.

The mechanism of epoxidation of propene has not been definitively determined, but a hydrogen peroxo-like species has been proposed as the oxidant. This proposal is based on several observations: (i) hydrogen peroxide is traditionally used as an oxidant in effective epoxidation of propene under mild conditions,[95] (ii) co-fed hydrogen is necessary in selective epoxidation of propene over supported gold catalysts, and (iii) hydrogen peroxide is produced by the reaction between hydrogen and oxygen in situ over the Au catalysts. It is also possible that atomic oxygen might promote epoxidation, as is the case on Ag catalysts; however, the low dissociation probability for O_2 would limit the rate of reaction.

Questions remain regarding the propene oxidation process promoted by supported Au nanocatalysts: (i) What components of the catalyst are active for the epoxidation—gold, the oxide support, or both? (ii) If both components are active, what are their respective roles? These questions are raised by the fact that only gold catalysts supported on TiO_2- or Ti-containing oxides promote selective propene epoxidation, but the details of propene oxidation over gold catalysts supported on those oxides are different. Even the necessity of gold particles for propene oxidation is brought into question since Ti-containing silica or silicate has activity for epoxidation both with and without gold particles. For example, selective epoxidation of propene in the presence of O_2 occurs over Ti-containing (34.5% of selectivity) or Ti- and Al-containing (30.6% of selectivity) hexagonal mesoporous silicas.[93] Ti-modified high silica zeolite with an Si/Al ratio of 1900 was also found to be effective for propene epoxidation with O_2 as an oxidant.[94] Titanosilicate (TS-1) was also found to catalyze epoxidation of propene using hydrogen peroxide as an oxidant.[95] In addition, the temperature where the selective propene epoxidation occurs is affected by the oxide support. When Au is supported on TiO_2, selective epoxidation only occurs below 373 K, whereas selectivity is maintained up to 473 K for titanosilicate supports, which results in higher conversion.[12]

The major difference between the two oxide supports is the presence of four-coordinated Ti sites in titanosilicates due to formation of isolated Ti^{4+} sites in the SiO_2 matrix. Notably, the Au particle size distribution was similar for TiO_2 and titanosilicate (2−5 nm average diameter).[12] It is well known that atomically dispersed Ti with tetrahedral coordination is present when the TiO_2 concentration is less than 15 wt % in high surface area catalysts.[97] TiO_2 crystallites phase separate at higher TiO_2 concentrations. Moreover, similar behavior has been visualized by STM using a model system where atomically dispersed Ti and TiO_x islands were formed on/in silica thin film grown on Mo(112) single-crystal surface (see Figure 8).[52] Ti-modified SiO_2 thin films were prepared by deposition of Ti onto a SiO_2 thin film at room temperature followed by oxidation and annealing. The morphology of this surface is strongly dependent on the Ti coverage (Figure 8), initially showing isolated bright spots on the terrace as well as at the step edges of the SiO_2 thin film at low Ti coverage (<10%) and the appearance of TiO_x islands on the terraces at the Ti coverages up to 20%. The isolated bright spots were attributed to the atomically implanted Ti by replacing Si atoms in the SiO_2 matrix, which form a local tetrahedral network within the SiO_2 matrix. More importantly, these four-coordinate Ti sites were demonstrated to be active nucleation sites for gold particles.[52] Recent DFT calculations also provide support for the assertion that tetrahedral Ti sites play a role as anchoring sites for Au clusters due to the introduction of low-lying empty levels with Ti 3d character in the silica gap. These states could hybridize with filled orbitals of the adsorbed Au atoms.[98] This electronic modification of gold particles by Ti sites on the support may, therefore, influence the reaction kinetics and/or reaction mechanism of propene epoxidation.

Alternatively, the tetrahedral Ti sites may serve as adsorption sites for the hydroperoxy intermediate, which is formed from the reaction between H_2 and O_2, or as sites for the reaction with propene on the SiO_2 matrix of the support.[12]

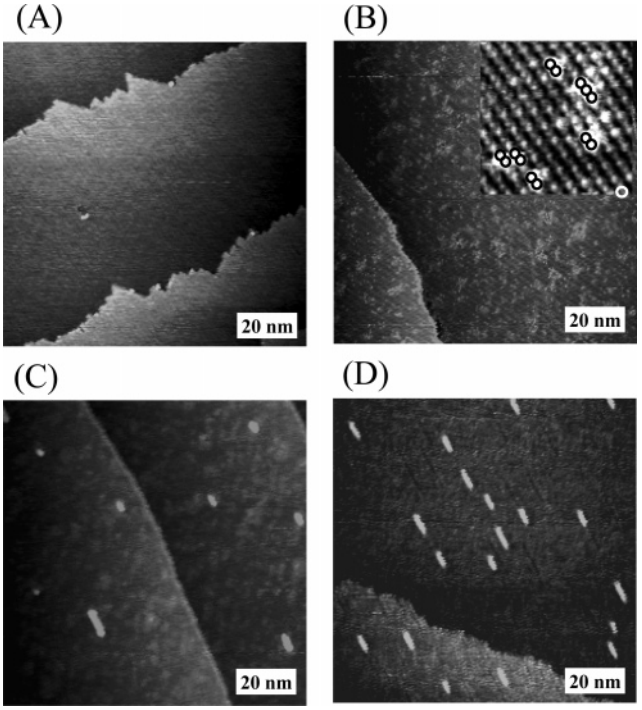

Figure 8. STM images (100 nm × 100 nm) of (A) clean SiO_2 thin film and (B, C, and D) Ti-modified SiO_2 thin films (TiO_2–SiO_2) with Ti coverages of 8%, 11%, and 17%, respectively. The inset of B shows an atomically resolved STM image (5.4 nm × 5.4 nm) where bright contrast spots indicate atomically substituted Ti in the silica lattice. Generally, the TiO_2–SiO_2 thin film shows initially atomically dispersed Ti sites followed by formation of TiO_x islands with the increase of Ti coverages. Reprinted with permission from ref 52. Copyright 2004 American Chemical Society.

This mechanism is different than the mechanism proposed for Au/TiO_2 catalysts, where molecular oxygen is taken up by a Ti^{3+} cation site to form hydroperoxo-like species directly through reaction with hydrogen.[12] The oxidant adsorbed on Ti sites is proposed to react with propene, which adsorbs on the gold particles.

There are still many questions regarding the important mechanisms and key features of the catalyst for propene epoxidation over Au supported on metal oxides. Because of the complexity of the catalyst system and the need for co-reactants, e.g., H_2 or H_2O, there is a need for model studies that can identify key factors controlling selectivity. Nevertheless, Au-based catalysts are clearly promising for commercial application of low-temperature and direct oxidation of propene to the epoxide.

2.2.2. Stability of the Gold Catalyst

Deactivation of gold catalysts is frequently observed under realistic reaction conditions. For example, in spite of initial high activity for CO oxidation, the activity of gold catalysts gradually decreases as a function of reaction time.[99] Deactivation of gold catalysts is generally attributed to either agglomeration of Au particles (sintering) or poisoning of active sites by accumulation of byproducts. Indeed, CO oxidation studied at high-pressure conditions (40 Torr) combined with STM studies using a Au/TiO_2 model system clearly showed that the activity of CO oxidation is diminished with respect to the reaction time accompanied with an increase of gold particle size. The sintering of the gold particles is thought to be facilitated by high pressures of O_2.[19] In addition to sintering, accumulation of a carbonate layer was also proposed for CO oxidation over high surface area Au/ZrO_2 catalysts. This carbonate layer blocks the access of new oxygen, leading to deactivation of the catalyst.[100]

Deactivation of the Au catalysts during propene oxidation ($T < 493$ K) occurred to a lesser extent when TiO_2 was incorporated into SiO_2 or other modified supports compared to TiO_2 itself, for which the propene oxidation activity was decreased during the first hours of operation. Although there was catalyst deactivation, sintering of the gold particles was *not* observed at the reaction temperature, implying that the poisoning of the active sites in the catalyst is the primary reason for deactivation of the gold catalyst in propene oxidation over these catalysts.[101] Furthermore, there is less deactivation at temperatures above 473 K, suggesting that either a strongly adsorbed species causes deactivation[102] or the barrier for diffusion of Au across the support is higher for the mixed TiO_2–SiO_2 support. The consensus is that the primary reason for deactivation for propene oxidation is poisoning by strongly bound byproducts not sintering.[101,102]

In order to probe for the possible formation of irreversibly bound species that may deactivate the catalyst, the interaction of both propene and propene oxide with the catalyst was investigated using IR spectroscopy.[103,104] While propene desorbs without reaction from the Au/TiO_2 catalyst, propene oxide reacts with acidic OH groups via an acid-catalyzed epoxide ring-opening reaction. A strongly bound bidentate, di-propoxy species forms, which leads to deactivation of the catalyst for propene oxidation.[101,103,105]

Oligomerization[106] or formation of carboxylates[105] from further oxidation of the bidentate propoxy intermediate was also proposed to lead to catalyst deactivation. In any case, it is generally agreed that this deactivation is due to blocking of active Ti sites on the TiO_2 surface by byproduct.[103] These results also provide a rationale for the better performance of Au catalysts supported on Ti-doped SiO_2 since Si sites in this oxide support are not active toward ring opening of propene oxide and Ti sites are highly dispersed; therefore, less bidentate di-propoxy intermediate is formed, and oligomerization is expected to occur to a lesser extent.[103,106]

3. Model Studies on Oxidized Au(111) Single Crystal

3.1. Oxidation of Au(111)

Model studies using Au(111) can provide insight into the intrinsic activity of Au in the absence of a support. Oxidized metal single-crystal surfaces have long been applied to surface science studies in order to gain fundamental insight into oxidative catalytic reactions.[107−110] Likewise, we and other groups have studied oxidation of CO and olefins (propene and styrene) promoted by oxidized gold single-crystal surfaces.[43,111−113] Since the dissociation probability for O_2 and NO_2 is low on gold single-crystal surfaces, other methods of oxidizing the Au surfaces under UHV conditions have been developed. For example, atomic oxygen has been prepared on Au(111) by exposure to ozone (O_3),[114] thermal dissociation of gaseous O_2 using hot filaments,[40,111] co-adsorption of NO_2 and H_2O,[115] application of a radio-frequency-generated plasma source,[116] electron bombardment on condensed NO_2,[41] and reactive ion sputtering with O_2^+.[117,118] It is important to note here that depending on the atomic oxygen preparation methods, the maximum oxygen coverages that can be reached are different. For example, ozone exposure to Au(111) yields oxygen coverages up to

1.2 ML[114] whereas electron-induced NO_2 dissociation or co-adsorption of NO_2 and H_2O only make about 0.4 ML as a maximum oxygen coverage.[41,115] In addition, the morphology of the surface and microscopic distribution of oxygen on the Au surface depends strongly on the method used for oxidation.

3.2. Formation of Metastable Oxygen Species on Au(111)

Oxidation of Au(111) leads to a release of Au atoms from the surface, leading to a rough surface morphology when oxidation is rapid (Figure 9). The net result is formation of oxidized Au nanoparticles on top of the Au(111) surface, thus eliminating interaction of Au with the support. Oxidation with ozone, which occurs rapidly, leads to formation of the oxidized Au nanoparticles on top of the surface (Figure 9).[113] Release of Au atoms upon oxidation is facilitated by the fact that clean Au(111) reconstructs to the well-known "herringbone" structure, which has an excess of 4.5% Au atoms compared to a bulk (111) plane, some of which are weakly bound at "elbow"sites.[119−121] Small perturbations in the surface, e.g., the presence of adsorbates, can alter the preferred structure of the surface.[121−124] As reviewed previously, the presence of excess Au in the surface layer provides a source of gold atoms that are released when electronegative atoms, e.g., O and S, release the surface stress when they are adsorbed on the surface.[42,120,125] Gold atoms may also be released from terraces, step edges, and dislocations to form mobile gold−oxygen complexes (Au−O) during oxidation, as reported for Cu(110) or Ni(110) surface.[126−128]

These islands or clusters formed from gold atoms released from the Au(111) surface during oxygen deposition may consist of either pure gold or gold−oxygen complexes, but the latter is more probable since gold atoms are expected to be very mobile at the temperature ranges used in the studies (200−400 K) and would be expected to diffuse to step edges. The apparent height of islands in both surfaces is close to that of the step height of clean Au, indicating formation of two-dimensional (2D) islands (Figure 9).[113] A narrow size distribution with the majority of islands having diameters between 1−5 nm is measured following oxidation with ozone at 200 K.

The size distribution and microscopic structure of the oxidized gold islands depends on the temperature used for oxidation. Larger islands with a broader size distribution were formed after oxidation at a surface temperature of 400 K compared to oxidation at 200 K even though the same ozone flux was used to render the same rate of oxidation (Figure 9).[113] This difference is attributed to the greater mobility of Au and Au−O complexes at 400 K and the greater stability of the larger and more ordered islands. Importantly, some of the islands formed by oxidation with ozone at 400 K have an ordered structure on an atomic scale over the length scales of 10−20 nm. For example, an ordered (1 × 3) structure is observed with both low-energy electron diffraction (LEED) and STM after deposition of 0.3 ML of oxygen via ozone decomposition at 400 K.[129]

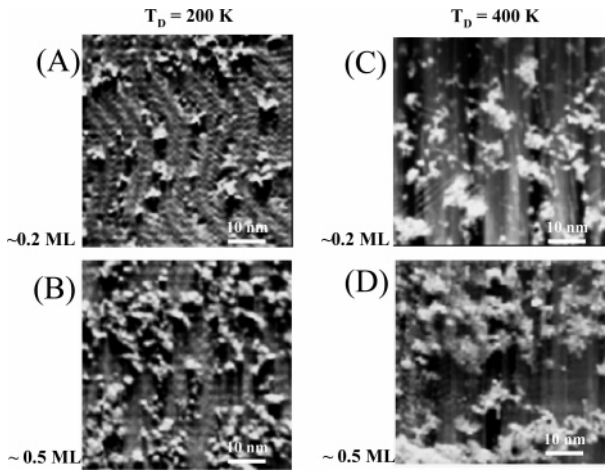

Figure 9. Scanning tunneling microscopic images (50 nm × 50 nm) of oxidized Au(111) surfaces where oxygen was deposited at 200 (A and B) and 400 K (C and D) using ozone.[113]

The local bonding characteristics of atomic oxygen also depend on the coverage and surface temperature used for oxidation based on interpretation of results of X-ray photoelectron and vibrational spectroscopic studies. Three distinct types of oxygen were tentatively identified: (1) chemisorbed oxygen, (2) surface oxide, and (3) bulk oxide.[129] The oxygen defined as chemisorbed does not have long-range order and consists of mobile Au−O complexes and disordered Au−O clusters that are ~5 nm in diameter. The well-ordered two-dimensional Au−O phase observed when oxidation is carried out using O_3 at 400 K is defined as a surface oxide, in analogy to the added row structures of oxygen on Ni(110) and Cu(110).[127,128] The bulk oxide contains oxygen in ordered, three-dimensional structures containing lattice oxygen.

The "chemisorbed" Au−O phase is metastable and converts to the more ordered phase upon heating. It also has high activity for both CO and olefin oxidation, as described below. The small (≤5 nm diameter), disordered Au−O islands form predominantly at low coverages of oxygen ($\theta_O \leq 0.5$ ML) for oxidation temperatures below 300 K. Heating to 400 K leads to an increase in the size of the islands and formation of the ordered 2-D oxide, even for coverages below 0.5 ML. The 3-D oxide is formed at higher coverages (($\theta_O \approx 1$ML), even when low oxidation temperatures are used.

The metastable nature of the nanoscale Au−O clusters containing "chemisorbed" oxygen is further illustrated by the fact that they are only formed when oxidation is carried out rapidly with O_3 decomposition at low temperature. If oxygen is deposited using electron-induced decomposition of NO_2, the Au released from the surface upon oxidation migrates to the step edge, yielding a smoother morphology and an ordered structure (e.g., (1 × 22)) on the terrace with the serrated step edge morphology, albeit a different structure from either the herringbone, characteristic of clean Au(111), or the (1 × 3) structure associated with the surface oxide formed from ozone decomposition.[42,129] These results indicate that there are several Au−O phases that can be accessed via kinetic control of the oxidation conditions.

The importance of the metastable Au−O phases formed on Au(111) is that, as described below in detail, it establishes the principle that metastable phases can be exploited for higher activity and higher selectivity than more stable phases. Since the metastable phase has a higher free energy than more stable phases, the energetics for oxidation will be lower for the metastable phase. Furthermore, these results provide strong evidence that care must be exercised in applying the results of theoretical calculations to understanding intrinsically kinetic processes since electronic structure calculations focus on the lowest energy binding state. In this vein, we also note that the ultrahigh vacuum studies do *not* probe for

possible reactivity of molecular O_2 since O_2 does not have a sufficient lifetime on the surface under these conditions to probe for reaction.

Below we show how the activity and selectivity for metastable Au−O phases on Au(111) efficiently promote oxidation of CO and olefins under UHV conditions. Accordingly, we establish that Au itself, even in the absence of a metal oxide support, is active for oxidation reactions, suggesting that one of the most important roles of the oxide support is to anchor and stabilize nanoscopic Au clusters that are also active for O_2 dissociation. Indeed, recent studies of catalytic CO oxidation by free-standing nanoporous Au foams corroborate that the support is not necessary for oxidation processes to be sustained over Au.[130] These results do not rule out secondary effects of the Au−support interaction that may have a role in determining selectivity, but they do establish the efficacy of undercoordinated Au itself for oxidation processes.

3.3. CO Oxidation Using an Oxidized Au(111)

Carbon monoxide is efficiently oxidized by atomic oxygen bound to several Au surfaces.[39,43−46] Furthermore, the reaction rate is highest around 200 K under UHV conditions, with a fall off with both increasing and decreasing surface temperature.[39,43−45] Specifically, CO oxidation on the Au(110) surface,[43] where oxygen atoms were prepared by electron bombardment of physisorbed O_2, showed an increase of the initial reaction rate between 60 and 180 K followed by a decrease up to 400 K, showing the highest initial reaction rate at a temperature of 180 K. Similar results also have been observed for oxidized Au(110), where oxygen atoms were prepared by exposure of oxygen through a Pt filament.[45] Likewise, the highest initial rate of reaction is observed at ∼200 K when Au(111) is oxidized at 200 K using ozone decomposition.[129] A similar dependence of the CO oxidation rate on reaction temperature was also reported for small gold particles oxidized using a hot filament to dissociate O_2—the highest rate was observed at 180 K followed by the decrease in initial rate with respect to the increase of reaction temperature.[39]

The rate decrease above 200 K is unusual since the rate constant (k_d) of a reaction is generally expected to increase with respect to temperature. The decrease in the rate of CO_2 production for reaction temperatures above 200 K is partly attributed to a decrease in the CO residence time with increasing temperature;[43,44] however, the distribution of oxygen on the surface also affects the rate. In the case of CO oxidation promoted by oxidized Au(111), we specifically show that the metastable oxygen phase is most active.

The importance of the oxygen distribution and bonding on the surface is apparent in studies of the dependence of the CO oxidation rate on the initial oxygen coverage. Generally, the rate of CO_2 production is expected to linearly depend on the coverage of oxygen and the availability of CO on the surface. If the oxygen coverage is fixed, the rate of CO_2 production would, thus, depend on the availability of CO and the temperature dependence in the reaction rate if all oxygen species are equally reactive. The residence time of CO on the surface, τ, can be estimated using the desorption characteristics of CO and the equation

$$\tau = k_d(\mathrm{T})^{-1} = [A \exp(-E_d/RT)]^{-1}$$

where A is pre-exponential factor and E_d is the activation energy of CO desorption. Clearly, the residence time of CO will decrease with temperature, contributing to the decrease in rate.

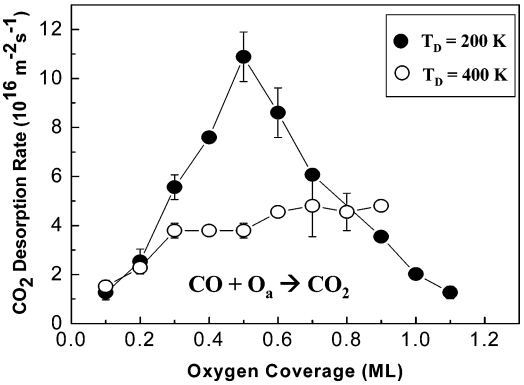

Figure 10. Initial rate of CO_2 production as a function of oxygen coverage deposited at 200 (filled circles) and 400 K (open circles). The initial reaction rate was determined by the initial increase of CO_2 desorption due to CO oxidation in the mass spectrometer normalized by the total area of CO_2 desorption profile for 300 s, which can be converted to absolute number of CO_2 molecules per area and time (atoms/m^2 s), assuming that 1 ML of CO_2 corresponds to the number of gold atoms on the Au(111) surface (1.3×10^{19} atoms/m^2).[129]

In order to further investigate the reactivity related to oxygen properties, oxygen atoms were prepared on Au(111) at two different temperatures—200 and 400 K—and subsequently the CO oxidation rate was measured at 200 K. Notably, 200 K is well above the CO_2 desorption temperature (100−120 K) on Au(111); thus, the rate of evolution of gaseous CO_2 is equal to the oxidation rate of CO.[43]

The initial rate of CO_2 production from CO oxidation at 200 K strongly depends on the surface temperature used for preparation of the oxygen layer (Figure 10). Furthermore, there is a significant difference in the dependence of the rate of CO_2 production on oxygen coverage for the two different temperatures used to prepare the oxygen overlayer (Figure 10). At low oxygen coverages (<0.2 ML), the initial reaction rate increases with respect to oxygen coverages for both deposition temperatures. As the oxygen coverage is increased, the behavior of the two surfaces diverges. The rate of CO_2 production increases linearly with increasing oxygen coverage up to 0.5 ML if the oxygen is deposited at 200 K, as expected. In contrast, the rate of CO_2 production is nearly independent of oxygen coverage if the oxygen layer was prepared at 400 K. At an oxygen coverage of 0.5 ML, the rate of CO_2 production for the oxygen layer deposited at 200 K is approximately a factor of 3 greater than for the oxygen layer created at 400 K, even though the temperature used for reaction is the same in both cases—200K.

The initial rate of CO oxidation on the O-covered surface prepared at 200 K reaches a maximum at 0.5 ML of oxygen. The initial rate of CO oxidation drops by an order of magnitude between 0.5 and 1.2 ML (saturation coverage) of oxygen deposited at 200 K. The decrease in rate may partly reflect the decrease in surface area available for CO adsorption; however, this does not fully explain all of the results. Notably, there is no change in the initial rate of CO oxidation over the same coverage range when the oxygen is deposited at 400 K. This result strongly implies that the nature and distribution of oxygen, which is determined by the conditions of oxidation, influences the CO oxidation rate.

As defined in the previous section, depending on the oxygen coverage and surface temperature, various oxygen

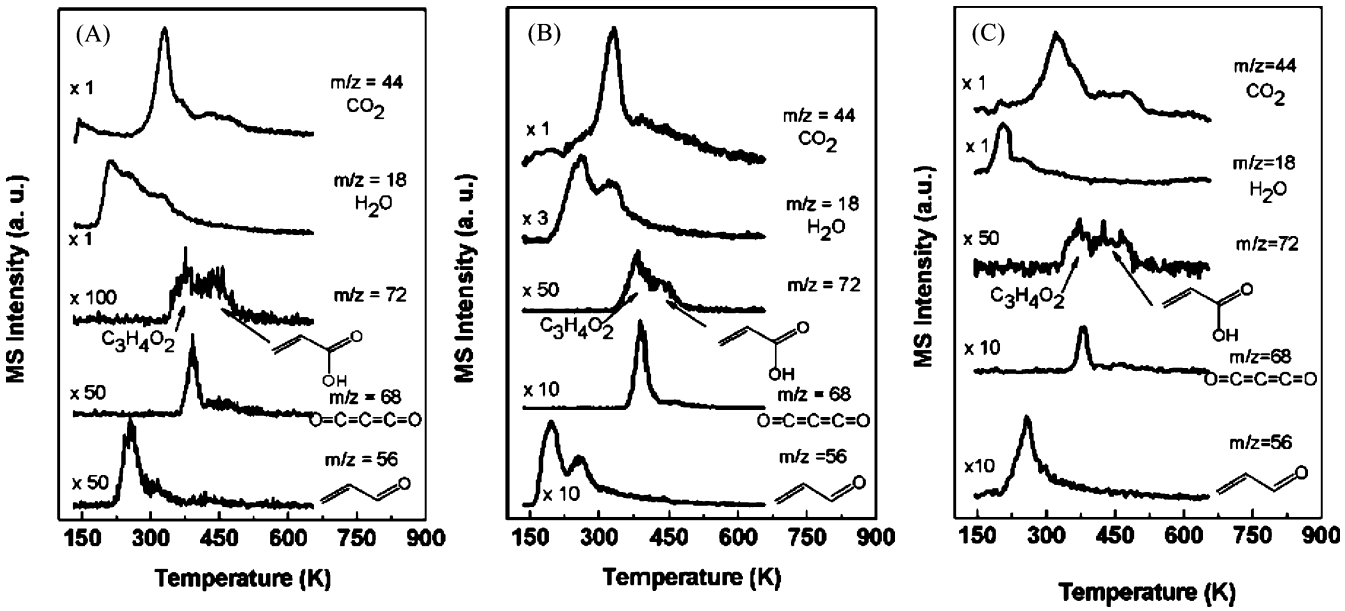

Figure 11. Temperature-programmed reaction spectra of (A) propene ($CH_3CH{=}CH_2$), (B) acrolein ($CH_2{=}CHCHO$), and (C) allyl alcohol ($CH_2{=}CHCH_2OH$) on oxygen-covered Au(111) ($\theta_O = 0.3$ ML). The data shown are the parent ion for each product. The oxygen-covered surface was prepared by exposing the surface to O_3 at 200 K. All reactants were adsorbed on the oxygen-covered Au(111) at 130 K with a pressure rise of 1×10^{-10} Torr for 30 s using direct dosing. Reprinted with permission from ref 113. Copyright 2006 American Chemical Society.

states (from chemisorbed to bulk oxide) were formed with respect to oxygen coverage deposited at 200 K, whereas larger islands with a well-ordered 2D structure attributed to a surface oxide formed when oxygen is deposited at 400 K. On the basis of the initial reaction rate for CO oxidation combined with characteristics of oxygen overlayer, we assert that metastable, chemisorbed oxygen species are more active for CO oxidation than the stable, ordered phase.

These results raise an important issue relevant to Au-based catalysis: metastable Au−O phases may play a role in determining activity or be used to enhance activity. Thus, the many factors that affect the CO oxidation rate—the presence of water, reaction pressure and temperature, Au particle size, and nature of the metal oxide support—may affect the nature of the oxygen species on the catalyst surface. On the basis of our studies on Au(111), the metastable, disordered phase of O is favored on small Au particles (2−5 nm in diameter). While it remains to be seen if metastable phases are available for reaction on supported Au catalysts under the conditions used for reaction, the concept of using metastable phases of oxygen to promote activity for, e.g., CO oxidation has general significance. By definition, metastable phases have a higher free energy than a stable phase; therefore, the energetics for reaction involving these phases will be lower than for a stable phase. Furthermore, metastable phases are more likely to be trapped at lower temperature where the mobility of surface species is limited, so that they are more likely to play a role in low-temperature processes. Conditions for catalytic activity would need to be optimized so as to sustain the transient, metastable phase during reaction. This might be accomplished by a pulsed reactor scheme.

3.4. Propene Oxidation Using an Oxidized Au(111)

The generality of exploiting metastable phases for enhancing activity for surface reactions is established by studies of propene oxidation. The metastable oxygen phase on oxidized Au(111) is also active for partial oxidation of propene, based on temperature-programmed reaction using atomic oxygen on Au(111) (Figure 11).[113] Specifically, atomic oxygen (0.3 ML) was prepared on Au(111) by exposure to ozone at 200 K followed by exposure to propene at 130 K. Although partial oxidation of propene is promoted by oxidized Au(111), the epoxide which is formed on supported Au nanocatalysts is not formed. It is possible that this difference might be due to an effect of the metal oxide support in the nanocatalysts. The products of partial oxidation of propene are acrolein, carbon suboxide, and acrylic acid (Figure 11A and Scheme 2). Combustion also occurs. Acrolein is evolved at 255 K, whereas other partial oxidation products are evolved at higher temperatures: 390 (carbon suboxide) and 440 K (acrylic acid). Parallel studies of allyl alcohol and acrolein provide insight into the reaction mechanism. Studies of allyl alcohol ($CH_2{=}CHCH_2OH$), which forms allyloxy, show that it also forms the same products, indicating that allyl oxy is formed from propene oxidation (Figure 11C). Isotopic labeling studies show that the allyloxy is formed from insertion into the allylic C−H bond of propene. Allyloxy is subsequently oxidized to acrolein. Evolution of gaseous acrolein competes with secondary oxidation to carbon suboxide, acrylic acid, and combustion products (Figure 11B). All partial oxidation products are evolved at the same temperatures and similar peak shapes to those from propene and acrolein oxidation: acrolein (255 K), carbon suboxide (390 K), and acrylic acid (440 K). The combustion peaks (CO_2 and H_2O) are also similar to those from propene oxidation.

As mentioned, epoxidation of ethene analogs has been widely observed in surface reactions of metal surfaces, but there is little evidence of selective epoxidation of propene in surface science studies except for the observation of some partial oxidation products (acetone and CO) in oxygen-covered Ag(111) surface.[131] A major reason for the low selectivity in propene oxidation by silver surface has been attributed to facile abstraction of allylic hydrogens by oxygen.

Scheme 2

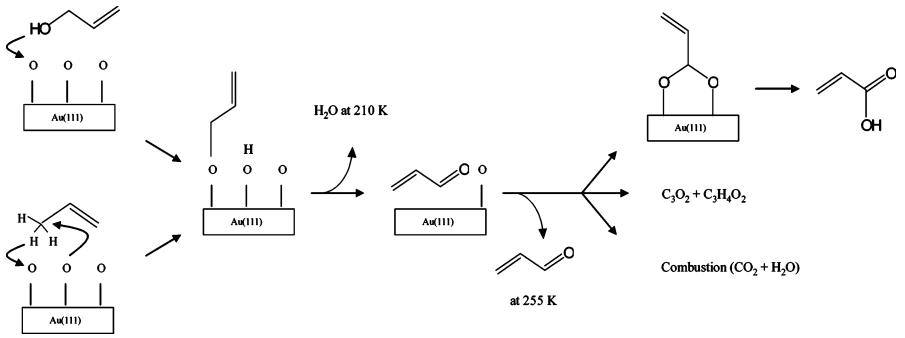

Similar to oxygen-covered silver, epoxidation of propene does not occur to any significant extent on oxygen-covered Au(111). However, acrolein is clearly produced by oxygen-covered Au(111), which is very different from Ag, where only combustion products were produced. Interestingly, acrolein was also produced by Au/SiO_2 high surface area catalyst (see Table 1) in propene oxidation.

The product distribution and activity for propene oxidation depend strongly on the conditions used for oxidation of the gold surface. The oxygen coverage, oxidation method, and oxidation temperature all effect the selectivity for propene oxidation, providing additional evidence that the distribution and local bonding of oxygen on the Au particles, even in the absence of a metal oxide support, is important for determining activity and selectivity. For example, the two different oxygen overlayers prepared on Au(111) by exposure to ozone at 200 and 400 K have different activities and selectivities with respect to propene oxidation. As described above, the gold surface oxidized at 200 K is considerably more active and yields partial oxidation products, whereas only combustion occurred on that prepared at 400 K. Furthermore, the activity for propene oxidation is higher when the surface is oxidized at 200 K. There is no residual oxygen on the surface when a saturation amount of propene reacts on a surface covered with 0.3 ML of oxygen prepared by oxidation at 200 K. In contrast, a substantial amount of oxygen (~46%) remains after reaction even though only combustion is observed. Taken together, these results demonstrate that metastable, disordered oxygen on Au is more active and more *selective* for propene oxidation, since the metastable phase is favored at low temperature.[129] Notably, the reaction product distribution is significantly different from previous studies of propene oxidation on Au(111) and Au(110), in which the reaction yielded major combustion products and a small amount of partial oxidation to products with $m/z = 56$ (possibly acrolein) and 58.[111] This difference may be due to different oxygen bonding resulting from the different method and surface temperature: atomic oxygen was created by passing O_2 over a glowing tungsten filament at 300 K.

Our studies of propene oxidation further illustrate that metastable oxygen phases on Au can be exploited to improve low-temperature activity and selectivity. It remains to be seen if this principle can be applied and exploited in actual catalytic processes. Nevertheless, the concept of using kinetically accessible phases to promote model studies of catalysis is established.

4. Summary and Perspectives

Gold-based catalysts are promising for efficient oxidation of CO and selective oxidation of propene. This is a fascinating set of catalytic processes because only nanoscopic gold is effective as a catalyst. These nanoscopic gold catalysts are active at much lower temperature compared to platinum-group catalysts for CO oxidation. Likewise, Au-based catalysts are effective for selective oxidation of propene, despite the very labile allylic hydrogen in this molecule.

Because of the complexity of the Au-based catalysts, there is significant debate regarding the underlying basis for the activity of these nanoscale materials. One important factor is that large Au particles and Au single crystals are not active for dissociation of O_2, which is likely to be a key step. Dissociation of O_2 is clearly related to the size and shape of gold particles and possibly to interactions with the water moiety and oxide support. Even the bonding of molecular oxygen (peroxo-type species), which has been proposed as a possible intermediate, is affected by the characteristics of Au. Model studies on oxidized Au(111) demonstrate, however, that atomic oxygen is very active for low-temperature oxidation of CO. These model studies further demonstrate that the interaction of Au with the metal oxide support is not necessary to impart activity to the Au and that metastable oxygen phases are particularly active at low temperature. At the same time, there is still a need to determine which features of the catalyst determine the long-term stability of the Au nanoparticles so that practical improvements can be made for improvement in, e.g., automotive catalysts.

Propene oxidation by gold catalyst is less well understood, in part because of the complexity of the reaction system. Metastable oxygen phases on Au(111) are active for partial oxidation of propene; however, acrolein, not the epoxide, is the primary oxidation product. While these model studies indicate that disordered phases of atomic oxygen are active for partial oxidation, there are still many unanswered questions as to how to efficiently promote epoxidation using Au-based nanocatalysts. Nevertheless, the efficient oxidation of propene—an important industrial process—might be achieved with Au-based nanocatalysts using O_2 as an oxidant.[132] Enhancing the stability of gold catalysts during propene oxidation is also a critical issue for future commercial application. Even though Ti-modified silica support is known to enhance the stability of gold catalyst, there is little understanding of the underlying basis of this phenomenon, demanding more systematic study with the assistance of a model system. This may enable further understanding the mechanism of propene oxidation by some special gold catalysts where gold particles are supported on TiO_2 or Ti-modified silica, which may help to design a more efficient gold catalyst for propene oxidation.

5. Acknowledgments

We gratefully acknowledge the partial support of this work by the U.S. Department of Energy, Basic Energy Sciences Program, under grant no. DE-FG02-84-ER-13289.

6. References

(1) Pattrick, G.; van der Lingen, E.; Corti, C. W.; Holliday, R. J.; Thompson, D. T. *Top. Catal.* **2004**, *30*−*31* (1−4), 273−279.
(2) Shelef, M.; Graham, G. W. *Catal. Rev.*−Sci. Eng. **1994**, *36* (3), 433−457.
(3) Hoebink, J.; van Gemert, R. A.; van den Tillaart, J. A. A.; Marin, G. B. *Chem. Eng. Sci.* **2000**, *55* (9), 1573−1581.
(4) Angelici, R. J. *Acc. Chem. Res.* **1988**, *21*, 387−394.
(5) Barteau, M. A. *Top. Catal.* **2003**, *22* (1−2), 3−8.
(6) Hutchings, G. J. *Catal. Lett.* **2001**, *75* (1−2), 1−12.
(7) Haruta, M.; Yamada, N.; Kobayashi, T.; Iijima, S. *J. Catal.* **1989**, *115* (2), 301−309.
(8) Hayashi, T.; Tanaka, K.; Haruta, M. *J. Catal.* **1998**, *178* (2), 566−575.
(9) Campbell, C. T. *Science* **2004**, *306* (5694), 234−235.
(10) Corti, C. W.; Holliday, R. J.; Thompson, D. T. *Appl. Catal. A: Gen.* **2005**, *291* (1−2), 253−261.
(11) Haruta, M. *Catal. Today* **1997**, *36* (1), 153−166.
(12) Sinha, A. K.; Seelan, S.; Tsubota, S.; Haruta, M. *Top. Catal.* **2004**, *29* (3−4), 95−102.
(13) Nijhuis, T. A.; Makkee, M.; Moulijn, J. A.; Weckhuysen, B. M. *Ind. Eng. Chem. Res.* **2006**, *45* (10), 3447−3459.
(14) Clark, H. W.; Bowman, R. G.; Maj, J. J.; Bare, S. R.; Ellyn, G. I.; Hartwell, G. E. U.S. Patent 5,965,754, 1999.
(15) Corti, C. W.; Holliday, R. J.; Thompson, D. T. *Gold Bull.* **2002**, *35* (4), 111−136.
(16) Okumura, M.; Nakamura, S.; Tsubota, S.; Nakamura, T.; Azuma, M.; Haruta, M. *Catal. Lett.* **1998**, *51* (1−2), 53−58.
(17) Bamwenda, G. R.; Tsubota, S.; Nakamura, T.; Haruta, M. *Catal. Lett.* **1997**, *44* (1−2), 83−87.
(18) Valden, M.; Lai, X.; Goodman, D. W. *Science* **1998**, *281*, 1647−1650.
(19) Valden, M.; Pak, S.; Lai, X.; Goodman, D. W. *Catal. Lett.* **1998**, *56* (1), 7−10.
(20) Iizuka, Y.; Tode, T.; Takao, T.; Yatsu, K.; Takeuchi, T.; Tsubota, S.; Haruta, M. *J. Catal.* **1999**, *187* (1), 50−58.
(21) Lopez, N.; Janssens, T. V. W.; Clausen, B. S.; Xu, Y.; Mavrikakis, M.; Bligaard, T.; Norskov, J. K. *J. Catal.* **2004**, *223* (1), 232−235.
(22) Comotti, M.; Li, W. C.; Spliethoff, B.; Schuth, F. *J. Am. Chem. Soc.* **2006**, *128* (3), 917−924.
(23) Schubert, M. M.; Hackenberg, S.; van Veen, A. C.; Muhler, M.; Plzak, V.; Behm, R. J. *J. Catal.* **2001**, *197* (1), 113−122.
(24) Chen, M. S.; Goodman, D. W. *Science* **2004**, *306* (5694), 252−255.
(25) Lemire, C.; Meyer, R.; Shaikhutdinov, S.; Freund, H. J. *Angew. Chem., Int. Ed.* **2004**, *43* (1), 118−121.
(26) Meier, D. C.; Goodman, D. W. *J. Am. Chem. Soc.* **2004**, *126* (6), 1892−1899.
(27) Kim, T. S.; Stiehl, J. D.; Reeves, C. T.; Meyer, R. J.; Mullins, C. B. *J. Am. Chem. Soc.* **2003**, *125* (8), 2018−2019.
(28) Remediakis, I. N.; Lopez, N.; Norskov, J. K. *Appl. Catal. A* **2005**, *291* (1−2), 13−20.
(29) Lemire, C.; Meyer, R.; Shaikhutdinov, S. K.; Freund, H. J. *Surf. Sci.* **2004**, *552* (1−3), 27−34.
(30) Janssens, T. V. W.; Carlsson, A.; Puig-Molina, A.; Clausen, B. S. *J. Catal.* **2006**, *240* (2), 108−113.
(31) Mavrikakis, M.; Stoltze, P.; Norskov, J. K. *Catal. Lett.* **2000**, *64* (2−4), 101−106.
(32) Engel, T.; Ertl, G. *Chem. Phys. Lett.* **1978**, *54* (1), 95−98.
(33) Cisternas, J.; Holmes, P.; Kevrekidis, I. G.; Li, X. J. *J. Chem. Phys.* **2003**, *118* (7), 3312−3328.
(34) Baxter, R. J.; Hu, P. *J. Chem. Phys.* **2002**, *116* (11), 4379−4381.
(35) Hopstaken, M. J. P.; Niemantsverdriet, J. W. *J. Chem. Phys.* **2000**, *113* (13), 5457−5465.
(36) Savchenko, V. I.; Boreskov, G. K.; Kalinkin, A. V.; Salanov, A. N. *Kinet. Catal.* **1983**, *24* (5), 983−990.
(37) Gottfried, J. M.; Schmidt, K. J.; Schroeder, S. L. M.; Christmann, K. *Surf. Sci.* **2003**, *536* (1−3), 206−224.
(38) Sault, A. G.; Madix, R. J.; Campbell, C. T. *Surf. Sci.* **1986**, *169* (2−3), 347−356.
(39) Kim, J.; Dohnalek, Z.; Kay, B. D. *J. Am. Chem. Soc.* **2005**, *127* (42), 14592−14593.
(40) Canning, N. D. S.; Outka, D.; Madix, R. J. *Surf. Sci.* **1984**, *141* (1), 240−254.
(41) Deng, X. Y.; Min, B. K.; Guloy, A.; Friend, C. M. *J. Am. Chem. Soc.* **2005**, *127* (25), 9267−9270.
(42) Min, B. K.; Deng, X.; Pinnaduwage, D.; Schalek, R.; Friend, C. M. *Phys. Rev. B* **2005**, *72* (12), 121410.
(43) Gottfried, J. M.; Christmann, K. *Surf. Sci.* **2004**, *566*, 1112−1117.
(44) Min, B. K.; Alemozafar, A. R.; Pinnaduwage, D.; Deng, X.; Friend, C. M. *J. Phys. Chem. B* **2006**, *110* (40), 19833−19838.
(45) Outka, D. A.; Madix, R. J. *Surf. Sci.* **1987**, *179* (2−3), 351−360.
(46) Lim, D. C.; Lopez-Salido, I.; Dietsche, R.; Bubek, M.; Kim, Y. D. *Angew. Chem., Int. Ed.* **2006**, *45* (15), 2413−2415.
(47) Park, E. D.; Lee, J. S. *J. Catal.* **1999**, *186* (1), 1−11.
(48) Guzman, J.; Gates, B. C. *J. Am. Chem. Soc.* **2004**, *126* (9), 2672−2673.
(49) Guzman, J.; Gates, B. C. *J. Phys. Chem. B* **2003**, *107* (10), 2242−2248.
(50) Wahlstrom, E.; Lopez, N.; Schaub, R.; Thostrup, P.; Ronnau, A.; Africh, C.; Laegsgaard, E.; Norskov, J. K.; Besenbacher, F. *Phys. Rev. Lett.* **2003** *90*, 026101-1.
(51) Min, B. K.; Wallace, W. T.; Goodman, D. W. *Surf. Sci.* **2006**, *600* (2), L7−L11.
(52) Min, B. K.; Wallace, W. T.; Goodman, D. W. *J. Phys. Chem. B* **2004**, *108* (38), 14609−14615.
(53) Min, B. K.; Wallace, W. T.; Santra, A. K.; Goodman, D. W. *J. Phys. Chem. B* **2004**, *108* (42), 16339−16343.
(54) Santra, A. K.; Kolmakov, A.; Yang, F.; Goodman, D. W. *Jpn. J. Appl. Phys 1* **2003**, *42* (7B), 4795−4798.
(55) Parker, S. C.; Grant, A. W.; Bondzie, V. A.; Campbell, C. T. *Surf. Sci.* **1999**, *441* (1), 10−20.
(56) Starr, D. E.; Shaikhutdinov, S. K.; Freund, H. J. *Top. Catal.* **2005**, *36* (1−4), 33−41.
(57) Spiridis, N.; Haber, J.; Korecki, J. *Vacuum* **2001**, *63* (1−2), 99−105.
(58) Shaikhutdinov, S. K.; Meyer, R.; Naschitzki, M.; Baumer, M.; Freund, H. J. *Catal. Lett.* **2003**, *86* (4), 211−219.
(59) Yoon, B.; Hakkinen, H.; Landman, U.; Worz, A. S.; Antonietti, J. M.; Abbet, S.; Judai, K.; Heiz, U. *Science* **2005**, *307* (5708), 403−407.
(60) Sanchez, A.; Abbet, S.; Heiz, U.; Schneider, W.-D.; Hakkinen, H.; Barnett, R. N.; Landman, U. *J. Phys. Chem. A* **1999**, *103*, 9573−9578.
(61) Goodman, D. W. *Catal. Lett.* **2005**, *99* (1−2), 1−4.
(62) Chen, M.; Cai, Y.; Yan, Z.; Goodman, D. W. *J. Am. Chem. Soc.* **2006**, *128* (19), 6341−6346.
(63) Minato, T.; Susaki, T.; Shiraki, S.; Kato, H. S.; Kawai, M.; Aika, K. I. *Surf. Sci.* **2004**, *566*, 1012−1017.
(64) Vijay, A.; Mills, G.; Metiu, H. *J. Chem. Phys.* **2003**, *118* (14), 6536−6551.
(65) Wang, Y.; Hwang, G. S. *Surf. Sci.* **2003**, *542* (1−2), 72−80.
(66) Vittadini, A.; Selloni, A. *J. Chem. Phys.* **2002**, *117* (1), 353−361.
(67) Okazaki, K.; Morikawa, Y.; Tanaka, S.; Tanaka, K.; Kohyama, M. *Phys. Rev. B* **2004**, *69* (23), 235404.
(68) Kim, Y. D.; Fischer, M.; Gantefor, G. *Chem. Phys. Lett.* **2003**, *377* (1−2), 170−176.
(69) Wallace, W. T.; Whetten, R. L. *J. Am. Chem. Soc.* **2002**, *124* (25), 7499−7505.
(70) Stolcic, D.; Fischer, M.; Gantefor, G.; Kim, Y. D.; Sun, Q.; Jena, P. *J. Am. Chem. Soc.* **2003**, *125* (10), 2848−2849.
(71) Schubert, M. M.; Kahlich, M. J.; Gasteiger, H. A.; Behm, R. J. *J. Power Sources* **1999**, *84* (2), 175−182.
(72) Grunwaldt, J. D.; Baiker, A. *J. Phys. Chem. B* **1999**, *103* (6), 1002−1012.
(73) Molina, L. M.; Rasmussen, M. D.; Hammer, B. *J. Chem. Phys.* **2004**, *120* (16), 7673−7680.
(74) Molina, L. M.; Hammer, B. *Appl. Catal. A* **2005**, *291* (1−2), 21−31.
(75) Remediakis, I. N.; Lopez, N.; Norskov, J. K. *Angew. Chem., Int. Ed.* **2005**, *44* (12), 1824−1826.
(76) Molina, L. M.; Hammer, B. *Phys. Rev. Lett.* **2003**, *90* (20).
(77) Liu, Z. P.; Gong, X. Q.; Kohanoff, J.; Sanchez, C.; Hu, P. *Phys. Rev. Lett.* **2003**, *91* (26).
(78) Liu, L. M.; McAllister, B.; Ye, H. Q.; Hu, P. *J. Am. Chem. Soc.* **2006**, *128* (12), 4017−4022.
(79) Date, M.; Okumura, M.; Tsubota, S.; Haruta, M. *Angew. Chem., Int. Ed.* **2004**, *43* (16), 2129−2132.
(80) Date, M.; Haruta, M. *J. Catal.* **2001**, *201* (2), 221−224.
(81) Bongiorno, A.; Landman, U. *Phys. Rev. Lett.* **2005**, *95* (10), 106102.
(82) Costello, C. K.; Yang, J. H.; Law, H. Y.; Wang, Y.; Lin, J. N.; Marks, L. D.; Kung, M. C.; Kung, H. H. *Appl. Catal. A* **2003**, *243* (1), 15−24.
(83) Boccuzzi, F.; Chiorino, A.; Manzoli, M.; Lu, P.; Akita, T.; Ichikawa, S.; Haruta, M. *J. Catal.* **2001**, *202* (2), 256−267.
(84) Liu, H.; Kozlov, A. I.; Kozlova, A. P.; Shido, T.; Asakura, K.; Iwasawa, Y. *J. Catal.* **1999**, *185* (2), 252−264.
(85) Mills, G.; Gordon, M. S.; Metiu, H. *J. Chem. Phys.* **2003**, *118* (9), 4198−4205.

(86) Yoon, B.; Hakkinen, H.; Landman, U. *J. Phys. Chem. A* **2003**, *107* (20), 4066−4071.
(87) Guzman, J.; Carrettin, S.; Corma, A. *J. Am. Chem. Soc.* **2005**, *127* (10), 3286−3287.
(88) Xu, Y.; Mavrikakis, M. *J. Phys. Chem. B* **2003**, *107* (35), 9298−9307.
(89) Mavrikakis, M.; Hammer, B.; Norskov, J. K. *Phys. Rev. Lett.* **1998**, *81* (13), 2819−2822.
(90) Liu, Z. P.; Hu, P.; Alavi, A. *J. Am. Chem. Soc.* **2002**, *124* (49), 14770−14779.
(91) Hakkinen, H.; Landman, U. *J. Am. Chem. Soc.* **2001**, *123* (39), 9704−9705.
(92) Grzybowska-Swierkosz, B. *Catal. Today* **2006**, *112* (1−4), 3−7.
(93) Liu, Y. Y.; Murata, K.; Inaba, M.; Mimura, N. *Catal. Lett.* **2003**, *89* (1−2), 49−53.
(94) Murata, K.; Kiyozumi, Y. *Chem. Commun.* **2001**, (15), 1356−1357.
(95) Clerici, M. G.; Bellussi, G.; Romano, U. *J. Catal.* **1991**, *129* (1), 159−167.
(96) Taylor, B.; Lauterbach, J.; Delgass, W. N. *Appl. Catal. A* **2005**, *291* (1−2), 188−198.
(97) Gao, X. T.; Wachs, I. E. *Catal. Today* **1999**, *51* (2), 233−254.
(98) Giordano, L.; Del Vitto, A.; Pacchioni, G. *J. Chem. Phys.* **2006**, *124* (3).
(99) Schubert, M. M.; Plzak, V.; Garche, J.; Behm, R. J. *Catal. Lett.* **2001**, *76* (3−4), 143−150.
(100) Konova, P.; Naydenov, A.; Tabakova, T.; Mehandjiev, D. *Catal. Commun.* **2004**, *5* (9), 537−542.
(101) Nijhuis, T. A.; Weckhuysen, B. M. *Chem. Commun.* **2005**, *48*, 6002−6004.
(102) Stangland, E. E.; Stavens, K. B.; Andres, R. P.; Delgass, W. N. *J. Catal.* **2000**, *191* (2), 332−347.
(103) Mul, G.; Zwijnenburg, A.; van der Linden, B.; Makkee, M.; Moulijn, J. A. *J. Catal.* **2001**, *201* (1), 128−137.
(104) Nijhuis, T. A.; Visser, T.; Weckhuysen, B. M. *J. Phys. Chem. B* **2005**, *109* (41), 19309−19319.
(105) Nijhuis, T. A. R.; Visser, T.; Weckhuysen, B. M. *Angew. Chem., Int. Ed.* **2005**, *44* (7), 1115−1118.
(106) Nijhuis, T. A.; Huizinga, B. J.; Makkee, M.; Moulijn, J. A. *Ind. Eng. Chem. Res.* **1999**, *38* (3), 884−891.
(107) Bol, C. W. J.; Friend, C. M. *Surf. Sci. Lett.* **1995**, *322*, L271−L274.
(108) Chan, A. S. Y.; Deiner, L. J.; Friend, C. M. *J. Phys. Chem. B* **2002**, *106* (51), 13318−13325.
(109) Roberts, J. T.; Capote, A. J.; Madix, R. J. *Surf. Sci.* **1991**, *253* (1−3), 13−23.
(110) Webb, M. J.; Driver, S. M.; King, D. A. *J. Phys. Chem. B* **2004**, *108* (6), 1955−1961.
(111) Davis, K. A.; Goodman, D. W. *J. Phys. Chem. B* **2000**, *104* (35), 8557−8562.
(112) Deng, X.; Friend, C. M. *J. Am. Chem. Soc.* **2005**, *127* (49), 17178−17179.
(113) Deng, X. Y.; Min, B. K.; Liu, X. Y.; Friend, C. M. *J. Phys. Chem. B* **2006**, *110* (32), 15982−15987.
(114) Saliba, N.; Parker, D. H.; Koel, B. E. *Surf. Sci.* **1998**, *410* (2−3), 270−282.
(115) Wang, J.; Voss, M. R.; Busse, H.; Koel, B. E. *J. Phys. Chem. B* **1998**, *102* (24), 4693−4696.
(116) Stiehl, J. D.; Kim, T. S.; McClure, S. M.; Mullins, C. B. *J. Am. Chem. Soc.* **2004**, *126* (42), 13574−13575.
(117) Gottfried, J. M.; Elghobashi, N.; Schroeder, S. L. M.; Christmann, K. *Surf. Sci.* **2003**, *523* (1−2), 89−102.
(118) Biener, M. M.; Biener, J.; Friend, C. M. *Surf. Sci.* **2005**, *590* (2−3), L259−L265.
(119) Narasimhan, S.; Vanderbilt, D. *Phys. Rev. Lett.* **1992**, *69* (10), 1564−1567.
(120) Bach, C. E.; Giesen, M.; Ibach, H.; Einstein, T. L. *Phys. Rev. Lett.* **1997**, *78* (22), 4225−4228.
(121) Ibach, H. *J. Vac. Sci. Technol. A* **1994**, *12* (4), 2240−2243.
(122) Biener, M. M.; Biener, J.; Friend, C. M. *Langmuir* **2005**, *21* (5), 1668−1671.
(123) Ibach, H.; Bach, C. E.; Giesen, M.; Grossmann, A. *Surf. Sci.* **1997**, *375* (1), 107−119.
(124) Sander, D.; Linke, U.; Ibach, H. *Surf. Sci.* **1992**, *272* (1−3), 318−325.
(125) Min, B. K.; Alemozafar, A. R.; Biener, M. M.; Biener, J.; Friend, C. M. *Top. Catal.* **2005**, *36* (1−4), 77−90.
(126) Besenbacher, F.; Norskov, J. K. *Prog. Surf. Sci.* **1993**, *44* (1), 5−66.
(127) Crew, W. W.; Madix, R. J. *Surf. Sci.* **1996**, *356* (1−3), 1−18.
(128) Crew, W. W.; Madix, R. J. *Surf. Sci.* **1996**, *349* (3), 275−293.
(129) Min, B. K.; Alemozafar, A. R.; Pinnaduwage, D.; Deng, X.; Friend, C. M. *J. Phys. Chem. B* **2006**, *110* (40), 19833−19838.
(130) Zielasek, V.; Jürgens, B.; Schulz, C.; Biener, J.; Biener, M. M.; Hamza, A. V.; Bäumer, M. *Angew. Chem., Int. Ed.* **2006**, *45* (48), 8241−8244.
(131) Huang, W. X.; White, J. M. *Catal. Lett.* **2002**, *84* (3−4), 143−146.
(132) Hughes, M. D.; Xu, Y. J.; Jenkins, P.; McMorn, P.; Landon, P.; Enache, D. I.; Carley, A. F.; Attard, G. A.; Hutchings, G. J.; King, F.; Stitt, E. H.; Johnston, P.; Griffin, K.; Kiely, C. J. *Nature* **2005**, *437* (7062), 1132−1135.
(133) Cant, N. W.; Hall, W. K. *J. Phys. Chem.* **1971**, *75* (19), 2914.
(134) Gasior, M.; Grzybowska, B.; Samson, K.; Ruszel, A.; Haber, J. *Catal. Today* **2004**, *91−92*, 131−135.
(135) Naito, S.; Tanimoto, M. *J. Chem. Soc., Faraday Trans. I* **1988**, *84*, 4115−4124.
(136) Chou, J.; Franklin, N. R.; Baeck, S. H.; Jaramillo, T. F.; McFarland, E. W. *Catal. Lett.* **2004**, *95* (3−4), 107−111.
(137) Haruta, M.; Tsubota, S.; Kobayashi, T.; Kageyama, H.; Genet, M. J.; Delmon, B. *J. Catal.* **1993**, *144* (1), 175−192.

CR050954D